Construction and Building Materials xxx (xxxx) xxx

Contents lists available at ScienceDirect

Construction and Building Materials

journal homepage: www.elsevier.com/locate/conbuildmat

Enhanced massivity index based on evidence from case studies: Towards a robust pre-design assessment of early-age thermal cracking risk and practical recommendations

Fragkoulis Kanavaris [a,*], Agnieszka Jędrzejewska [b], Ioannis P. Sfikas [c], Dirk Schlicke [d], Selmo Kuperman [e], Vít Šmilauer [f], Túlio Honório [g], Eduardo M.R. Fairbairn [h], Gabriella Valentim [h], Etore Funchal de Faria [i], Miguel Azenha [j]

[a] Specialist Technology & Research, Advanced Digital Engineering, ARUP, London, United Kingdom
[b] Silesian University of Technology, Department of Structural Engineering, Gliwice, Poland
[c] Asset Management Advisory, Strategic Consulting, Jacobs U.K. Ltd., London, United Kingdom
[d] Institute of Structural Concrete, Graz University of Technology, Graz, Austria
[e] Desek Ltd, Brazil
[f] Department of Mechanics, Faculty of Civil Engineering, Czech Technical University in Prague, Czech Republic
[g] Université Paris-Saclay, ENS Paris-Saclay, CNRS, LMT – Laboratoire de Mécaniqiue et Technologie, 94235 Cachan, France
[h] COPPE/UFRJ Civil Engineering Department of the Post-Graduate Institute of the Federal University of Rio de Janeiro, Brazil
[i] Itaipu Binacional, Civil Works Division, Brazil
[j] ISISE, University of Minho, Department of Civil Engineering, Campus of Azurém, Guimarães, Portugal

HIGHLIGHTS

- Case studies on thermal cracking of massive structures are analysed.
- Recommendations from forensic investigations on thermal cracking are given.
- Massive foundations, dams and columns are considered.
- The enhanced index can be used as pre-design assessment for thermal cracking.
- The method can be useful to designers/contractors dealing with massive structures.

ARTICLE INFO

Article history:
Received 12 April 2020
Received in revised form 22 October 2020
Accepted 30 October 2020
Available online xxxx

Keywords:
Mass concrete
Massivity index
Thermal cracking
Forensic engineering
Cracking risk
Foundation blocks
Armour units
Footings
Dams
Spillways

ABSTRACT

Tensile stresses resulting from a combination of thermal volumetric changes, due to the heat of hydration and ambient conditions, autogenous deformations and boundary restraints, often induce a significant intrinsic load on massive concrete structures. Whenever such stresses attain the concrete tensile strength, cracking occurs, which may in turn impair the serviceability and durability of the structure. This study is an output of Working Group 7 of RILEM Technical Committee 254-CMS: *Thermal cracking in massive concrete structures* and is presenting case studies of early-age thermal cracking in massive concrete structures where internal restraining conditions often prevail, such as thick blocks, armour units, footings, dams and spillways, and large-sized columns. It covers the analysis of causes of this type of cracking together with the lessons learned from the collected evidence along with best mitigation practices (often resulting from forensic investigations by means of computer-based simulations). Based on the evidence retrieved from the analysed case studies, the concept of massivity used to indicate potential thermal crack proneness in massive concrete structures is significantly improved to account for binder type and content as well as casting and fresh concrete temperature, in addition to the geometrical characteristics of the element under investigation. The use of such an indicator may lead to a more robust pre-design assessment of the likelihood for thermal cracking occurrence in massive concrete elements, advising designers and contractors dealing with such structures whether more complex analyses should be performed already at the design stage.

* Corresponding author.
E-mail address: frag.kanavaris@arup.com (F. Kanavaris).

https://doi.org/10.1016/j.conbuildmat.2020.121570
0950-0618/

1. Introduction

1.1. Scope of study

Serviceability limit state (SLS) of cracking in concrete structures due to imposed deformations, resulting from restrained thermal and shrinkage effects due to concrete hydration, hereinafter referred to as early-age cracking, has been a topic of ongoing concern and investigations for both designers and contractors and, consequently, researchers [1–8]. Apart from the negative effect on aesthetics, such cracks may also promote corrosion of the embedded reinforcing steel and ultimately impair the durability of a concrete structure [9] or may even be responsible for section load capacity reduction, as it will be discussed in this study. In specific types of concrete structures cracking can also considerably impair functionality. For example, early-age through-section cracking may be one of the primary causes of apparent leakage in liquid-retaining concrete structures [10,11], whilst in safety-critical nuclear structures air tightness and, hence, radiation resistance, are largely controlled through crack characteristics [12]. By this, additional and usually unexpected expenses to identify cracks, analyse the causes and for possibly required repair works are incurred [13], while the risk of high dispute costs and/or reputational damage to the parties involved in the design and construction can be substantial [14].

The types of massive concrete structures often impaired by early-age thermal cracking include, but are not limited to, massive foundation blocks and rafts, armour (breakwater) units, hydraulic structures such as sluices, dams and spillways and large-sized beams and columns (see Fig. 1). Due to the nature of the problem and the sensitive and often confidential information associated with it which restricts dissemination capability, the task to identify relevant examples in literature, also with adequate background information is challenging.

As part of the tasks of Working Group 7 of RILEM Technical Committee 254-CMS: *Thermal cracking in massive concrete structures*, case studies on early-age cracking in massive concrete structures have been collated following an extensive literature review and empirical methods for the characterisation of a massive concrete structure in terms of thermal cracking propensity have been reviewed and improved accordingly.

The study presented in this paper was based on a comparative analysis of a number of representative case studies of massive concrete structures, where mix compositions, casting and curing methods, environmental conditions and some fundamental material parameters were known. This overview also included studies where forensic analyses were conducted in order to identify or add confidence on the causes of cracking. The considered case studies were presented in detail in the Appendix to this paper with references to source material given to the reader wherever possible.

The main aim of the study, elaborated in Section 2, was critical evaluation of currently used tools for quantitative assessment of the structure's proneness to early-age thermal cracking followed by the proposal of an enhanced approach. The massivity concept - a simplistic approach for assessing the thermal cracking proneness of a massive concrete structure based on its geometry, - and its weaknesses were identified, discussed and analysed. This was then followed by proposed improvements to more representatively account for relevant phenomena and influencing factors, such as binder type/content and ambient temperature, with substantiation arising from the evidence collected from the case studies. The associated theoretical background and corresponding improvements were then presented in detail (Section 3). The last section of the paper (Section 4) includes major conclusions and key recommendations for best practice regarding design process of massive concrete structures.

1.2. Remarks on thermal cracking in massive concrete structures

While thermal cracking can be relevant to relatively thin sections in which rapid heat dissipation occurs and the risk of associated cracking is increased by simultaneous shrinkage effects, as discussed elsewhere [15–17], it is normally deemed more important for large concrete pours, due to the high, nearly adiabatic temperatures developed which can be also sustained for longer periods of time [15–25]. Unless the surfaces are well-insulated to restrict quicker cool-down than in the core, temperature differentials may create high thermal gradients (depending on element size and thermal properties of the mix, such as conductivity and heat transfer coefficient) and induce thermal stresses. This phenomenon is known in the literature as internal restraint and is mostly applicable to dimensionally significant structures, where also the effects of external restraint can be near-negligible.

Surface cracking due to internal restraint in massive concrete arises from the fact that, over the so-called heating period, the temperature in the core is greater than at the surfaces, leading to compressive stresses in the hot core and tensile stresses at the

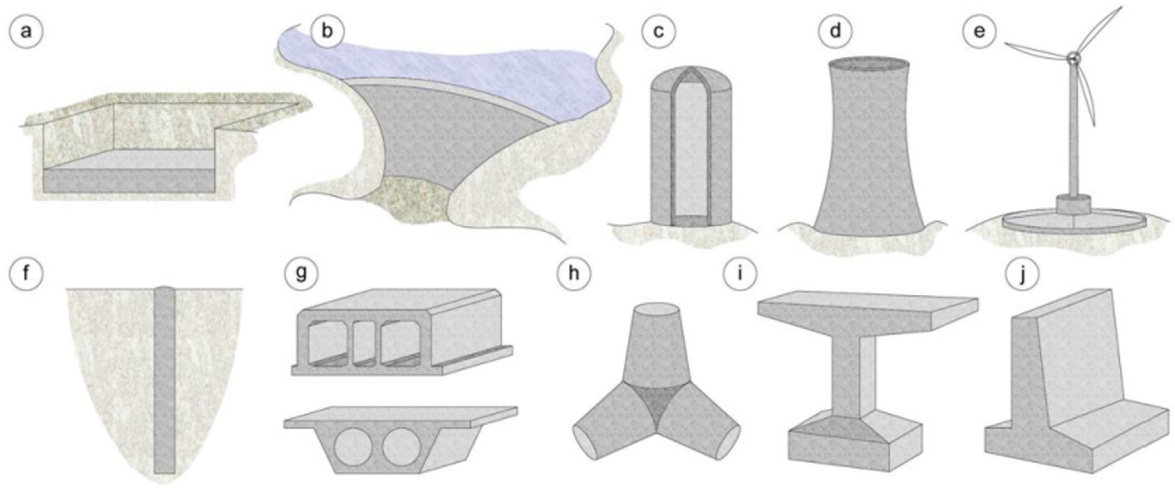

Fig. 1. Examples of concrete structures that often exhibit hardening-induced cracking: a) ground slabs, b) concrete dams, c) silos/containment structures, d) cooling towers, e) wind turbine foundations, f) piles, g) precast segments (top: immersed tunnel, bottom: bridge deck), h) armour units, i) bridge piers and (j) retaining walls [15].

cooler surfaces [10,11,22,24]. During the period of cooling to ambient temperature, an inversion of the stress distribution may occur, with compressive stresses at the surface and tensile stresses in the core. But the simple distinction between the surface and core must not be sufficient in very massive structures. As a result of thermal contraction of a surface-near region in between core and surface, which occurs before the actual cooling of the core, the previously formed surface cracks may reduce in width while cracks may propagate in the direction of the core of the section. These cracks are often deemed more detrimental to concrete durability [9]. In massive dam structures, cooling to ambient temperature may take several years and cracks may appear even years after construction. For example, in the case of Orlik dam construction in Czech Republic, 40 surface cracks up to width of 3 mm appeared after one year from casting with core and surface temperature being 40°C and close to zero, respectively, and a 3 m crack depth was reported [25]. If structures are large enough to generate thermal gradients due to hydration, but still as small so that external restraining effects cannot be ignored, such internally-restraining conditions can be combined with external restraint from stiff boundaries, such as the ground or adjacent concrete elements, and shrinkage-related effects, which can further exacerbate the magnitude of the generated stresses [10,11,16,17]. Nevertheless, such conditions are not in the scope of this study where focus is given to cases in which internal restraining conditions are dominant. The present study, therefore, pertains to self-equilibrated temperature differentials and stresses within the cross-section of an element which may result in surface cracking. This intentionally disregards any externally restraining conditions which might induce additional stresses and require a different analysis approach to that presented herein.

This investigation naturally excludes the effects of autogenous shrinkage and drying shrinkage as: a) concretes used in massive pours are usually medium to low strength and such concretes exhibit relatively low autogenous shrinkage – besides, this shrinkage mechanism is relevant when externally-restraining conditions prevail and b) drying shrinkage in massive concrete structures occurs very slowly and its effects are typically not significant and if significant, they may cause some superficial cracking due to moisture gradients.

Apart from thermal cracking due to internal or external restraint, high temperatures due to cement hydration also pose a significant risk of expansion and cracking due to delayed ettringite formation (DEF) [26]. DEF is a form of internal sulfate attack which is caused by the delayed formation of the mineral ettringite, regularly produced during hydration, when concrete temperature exceeds 65–80°C (it should be noted that this range is very much dependent on cement composition and cementitious materials used [26–28]). DEF is a consequence of high temperatures within concrete [29] related to expansive chemical reactions and in general, the stress generation due to restraining of herewith imposed deformations is subject to the same mechanical background. Anyhow, DEF was not in the scope of this study on cracking due to internal restraint and as such, although DEF is mentioned herein, it will not be examined thoroughly in the next sections. Further information can be found elsewhere, e.g. [30].

2. Evaluation of structure's proneness to thermal cracking

The considerations discussed in this paper are based on the evidence collected by the members of the RILEM TC 254-CMS and relate to 7 distinct, representative large-volume concrete structures in which hardening-induced cracking was reported. The structures in question are described in detail in subsequent section of the Appendix to this paper. For all considered case studies the observed cracking was predominately attributed to hardening-induced thermal stresses reaching the tensile capacity of concrete. These thermal stresses were formed in the volume of the elements due to temperature differentials caused by dissipation of heat that is generated by hydration of cement during hardening of these elements. High magnitude of thermal gradients was mainly caused by the combination of large dimensions of the structural elements and the material characteristics.

The risk of thermal cracking can be mitigated if appropriate measures are applied at the construction stage, which in turn may require that a detailed thermo–mechanical analysis (e.g., FEM-based) is performed early in the design process. Such analysis is not performed very often, it is, however, encouraging that it is gradually being adopted for big infrastructure projects, especially of higher significance [31]. One of the reasons for the limited application is the lack of clarity in guidelines regarding the classification of massive concrete structures. For example, ACI 116R [32] defines mass concrete as "*any volume of concrete with dimensions large enough to require that measures be taken to cope with generation of heat from hydration of the cement and attendant volume change to minimize cracking*". It is evident that the designer has to make a difficult, yet responsible decision about the potential risk of early-age thermal cracking in any large volume of concrete and the need of performing thermal analysis. This decision can be potentially aided through the concept of quantifying proneness to cracking using massivity indexes. Different approaches in evaluating the massivity that can be used to support this decision process are described in the following sections.

2.1. Characteristic length approach

One of the most complete approaches for evaluating the massivity of a structure is that proposed by *Ulm and Coussy* [33], which considers both the dimensions of the element and its thermo–physical properties. The concept of a "*characteristic length of hydration heat diffusion*", l_h [m], is introduced to determine the minimum dimensions above which, for a given material, a structure should be considered as massive, i.e. in which the heat of hydration is expected to significantly affect the overall thermo–chemo–mechanical behaviour. For Neumann boundary conditions and a semi-infinite domain the characteristic length, l_h [m], is defined as:

$$l_h = \sqrt{\frac{D}{A(\alpha)} exp\left[-\frac{E_a}{RT}\right]} \quad (1)$$

where:

D – thermal diffusivity, ratio between thermal conductivity and volumetric heat capacity;

$A(\alpha)$ – affinity function of the degree of hydration;

E_a – activation energy of binder;

R – universal gas constant;

T – absolute temperature.

Then for l being the maximum distance of any point within the structure to the nearest external surface:

- if $l \gg l_h$ the structure is classified as massive as heat dissipation from the structure is very limited and non-negligible thermal stresses may arise,
- if $l \ll l_h$ structure is classified as non-massive quick heat dissipation is permitted and
- if $l \approx l_h$ the occurrence of thermal gradients in the structure is probable.

This approach has three major implications. Firstly, detailed information about the thermo–physical properties of concrete are required prior to analysis to determine the value of the

characteristic length. Secondly, the formulation assumes that the characteristic length varies with the degree of hydration and with temperature. Then, in a range of structures, boundary conditions cannot be represented as Neumann-type and the approach may exhibit limited applicability [34].

2.2. Surface area approach

Other approaches exist that relate solely to the geometry of the element. It is generally established that the massivity of the element can be evaluated by relating its volume to the area of surfaces. The former impacts the magnitude of core temperature, whereas the latter impacts the temperature difference. Such an approach for the evaluation of massivity is proposed by ACI 207.2R [35]:

$$M = \frac{V}{S} \tag{2}$$

where:

- the volume V (m^3) is determined by summing the volume of concrete and additional concrete volume equivalent to the volume of insulation. It is suggested that the effect of steel forms is neglected as steel is a poor insulator while the thickness of wood forms or insulation in the direction of principal heat flow should be considered in terms of their affecting the rate of heat dissipation.
- the area S (m^2) represents the total area of surfaces through which heat dissipates. The expression "*total area of exposed surfaces*" can be also found in relevant literature (see e.g. [36]) which generates a degree of debate regarding the interpretation of this parameter. ACI 207.2 [35] specifies that any faces further apart than 20 times the thickness of the member can be ignored as contributing to heat flow, which applies easily to the elements of relatively small thickness with respect to the other two dimensions, such as walls. However, the question about the heat flow through the bottom surface of the element to the ground, which is very important in massive concrete elements such as foundation blocks or slabs, remains open.

2.3. Equivalent thickness approach

De Schutter and Taerwe [36] elaborated on the ACI concept of massivity and concluded that there is not always a unique relationship between the massivity and the maximum temperature / temperature gradient in the concrete element, especially for elements with complex geometry. Therefore, they proposed to use the equivalent thickness, d_{eq}, as a measure of massivity of the element, defined as a product of massivity calculated acc. to Eq. (2) and the shape factor of the heat flow area, γ_a:

$$d_{eq} = \gamma_a \cdot M \tag{3}$$

where the shape factor is a measure for the distance of the most inner point to the exposed surface relative to the distance of the centre of gravity to the exposed surface. Unfortunately, no boundary values are given based on which the structure can be classified as massive.

2.4. Surface modulus approach

In an alternative approach, recommendations are given by *Flaga* [37] who uses the so-called surface modulus defined as:

$$m_s = \frac{S}{V} \tag{4}$$

The surface modulus can be regarded as a reciprocal of the massivity defined by Eq. (2), however, a different approach is used to determine the values of the volume and area of surfaces. For the latter one, it is recommended to refer to the exposed surfaces only, although is not explicitly specified which surfaces should be regarded as exposed. In the referred work it is generally assumed that for block elements (i.e. the elements with all three dimensions of comparative values) all surfaces are treated as contributing to the heat flow while for the wall elements the total area is limited to the area of the wall faces. For the volume, only the volume of concrete is taken into consideration (no remarks on the effect of insulation are made). Following these assumptions concrete structures are divided into three groups, based on the surface modulus:

- for $m_s \leq 2 m^{-1}$ structures are classified as massive with a predominant impact of thermal strains and close-to-adiabatic conditions in the core;
- for $2 m^{-1} < m_s < 15 m^{-1}$ structures are classified as semi-massive with a comparable impact of thermal and drying shrinkage strains;
- for $m_s > 15 m^{-1}$ structures are classified as thin-walled concrete structures with negligible impact of thermal strains.

2.5. Comparison of different approaches

Although the concept of defining the massivity of concrete structures is generally established, there are discrepancies among the above-mentioned methods when defining relevant geometrical characteristics. Therefore, in this paper the following measures are indicated for each case:

1. **Basic Massivity** M_{basic} calculated as a ratio between the volume of concrete and total area of surfaces (not code-based): $M_{basic} = \frac{V_{concrete}}{S_{total}}$, [m].
2. **Massivity** M calculated as a ratio between substitute volume (volume of concrete + volume representing insulation layers) and total area of exposed surfaces (after ACI 207.2 [35]): $M = \frac{V_{total}}{S_p} = \frac{V_{concrete}+V_{ins}}{S_p}$, [m]. Heat flow to the ground is neglected (as contributing to the overall heat flow on much smaller magnitude than to the air).
3. **Equivalent thickness** d_{eq} calculated as a product of massivity M determined as per (2) above and shape factor after [36]: $d_{eq} = \gamma_a \cdot M$.
4. **Surface modulus** m_s calculated as a ratio of the total area of exposed surfaces and volume of concrete after [37]: $m_s = \frac{S_p}{V_{concrete}}$, [$m^{-1}$]. For the cases analysed in this paper all surfaces are treated as exposed surfaces $S_p = S_{total}$.

3. Applicability & recommendations on massivity concept

3.1. Application of current massivity indexes to case studies

The corresponding values of the proposed indexes of massivity were determined for all the cases discussed in the paper and are collectively presented in Table 1.

It can be concluded that almost all of the analysed structures were characterised with the surface modulus $m_s < 2\ m^{-1}$, and should therefore - according the proposal of [37] - be classified as massive. There was one case of concrete lifts characterised with the surface modulus of 2.2 m^{-1}, however, the overall surface modulus for the whole structure was $\ll 1\ m^{-1}$. The only case which did not follow this rule was a concrete armour unit for which the surface modulus was ranging between 2 and 2.8 m^{-1}, depending on

Table 1
Measures of massivities of the structures discussed in cases studies calculated based on different methods.

Structure type	Section No.	Dimensions [m]	M_{basic}[m]	M[m] [35]	d_{eq}[m] [36]	m_s[m^{-1}] [37]
Massive blocks, rafts and footings	A.1.1.	5 × 5 × 4.6	0.81	0.98	3.07	1.02
	A.1.2.	1.8 × 1.8 × 1.8	0.30	0.36	1.20	2.78
		2.2 × 2.2 × 1.6	0.33	0.41	1.07	2.44
		2.2 × 2.2 × 2.2	0.37	0.44	1.47	2.27
		2.5 × 2.5 × 2.5	0.42	0.50	1.67	2.00
	A.1.3.	18.5 × 6.1 × 1.83	0.65	1.02	1.22	0.98
		12.8 × 8.3 × 1.83	0.67	1.06	1.22	0.94
		28.4 × 18.6 × 4.5	1.61	2.50	3.00	0.40
		21.5 × 7.8 × 2.7	0.92	1.39	1.80	0.72
		6.0 × 7.0 × 2.5	0.70	0.98	1.67	1.02
Dams and spillways	A.2.1.	40 × 8 × 2.5	0.91	1.43	1.67	0.70
	A.2.2.	35 × 15 × 0.5 (lifts 1,2 & 3)	0.24	0.46	0.33	2.19
		35 × 15 × 2 (lifts 4, 5, 6)	0.84	1.45	1.33	0.69
		35 × 15 × 7.5 (whole structure)	2.19	3.09	5.00	0.32
	A.2.3.	17 × 36 × 85 (approx.)	3.96	3.96	56.67	0.25
Massive columns and piers	A.3.1	3.5 (d: diameter) × 8	0.60	0.65	2.63	1.54
		3.5 (d) × 10	0.64	0.81	2.63	1.23
		4.5 (d) × 7.5	0.71	0.98	3.38	1.02
		4.5 (d) × 9	0.76	1.18	3.38	0.85

the geometry of the block. The upper boundary value of the surface modulus m_s = 2 m^{-1} corresponds to the lower boundary value of basic massivity M_{basic} = 0.5 m, which is confirmed by the comparison (except for the limited number of cases discussed above), i.e. all structures characterised with M_{basic} > 0.5 m can be regarded as massive structures.

When analysing the massivity M determined according to recommendations of [35] considering an increased volume representing insulation and reduced heat flow to the ground, the limit value of massivity raises to the value of approximately 1, however, for some cases, which would otherwise be classified as massive (e.g. piers), this value is lower. Given the disputable assumption of neglecting the base surface as contributing to the overall heat flow it seems rational to assume also the lower boundary value of the massivity M = 0.5 m as a safe estimator of the massivity of concrete structures.

Having in mind the above, it seems obsolete to use the equivalent thickness as an engineering measure of massivity of concrete structures. Although a conclusion can be drawn from the presented comparative study that the equivalent thickness d_{eq} of at least 1 m should classify the structure as massive, determination of this value requires surplus work to be done in addition to determining sole massivity of the structure (since shape factor must be known). Therefore, given that the estimator of massivity should be a quick-to-obtain orientational value it seems more reasonable to refer to the massivity/surface modulus.

3.2. Proposed modifications and enhancements to the current massivity index

Currently, the massivity concept is a simple and relatively quick calculation of a thermal cracking potential of an element based solely on its geometrical characteristics. Nonetheless, it is well recognised that, although the geometry of the element governs heat dissipation, there are multiple other factors that play an important role in determination of risk of thermal cracking in massive concrete structures. Amidst the most influential of such factors may be considered the binder type and content and casting and ambient temperature throughout curing.

The incapability of the traditional massivity indexes to account for the previously mentioned factors reflects its incompleteness as a concept and implies that any thermal cracking risk approximation using this method may be relatively inaccurate. This section, therefore, aims to address these deficiencies of the massivity index through deriving correction factors which can be used to account for the aforementioned influential phenomena. It is the intention for the correction factors concept to maintain an engineering approach, thus upon their derivation, they can be simply applied to a massivity concept in order to obtain the enhanced massivity. It is suggested that the concept of surface modulus, m_s, i.e. section 2.4, is used and corrected since it also provides boundaries. As mentioned earlier, the proposed massivity modifications encompass the effects of binder type and content, casting and ambient temperature and temperature drop. As such, the enhanced massivity index can be obtained from:

$$M_{cor} = \frac{m_s}{k_f \times k_b \times k_{\Delta T}} \tag{5}$$

where k_f, k_b and $k_{\Delta T}$ are dimensionless correction factors accounting for cement type, binder content and temperature differential, respectively.

It is hoped that the corrections will, ultimately, enable the massivity index to be used reliably and reasonably conservatively by engineers during pre-design stages in order to determine the likelihood for thermal cracking and take better informed decisions on the depth of analysis required. The reasoning, justification and derivation of each correction factor individually is outlined in the subsections below. It should be mentioned that any effect reinforcement has in crack development, e.g. controlling the crack width and spacing, is not accounted for in the massivity concepts, which deal with cracking risk rather than crack characteristics. Furthermore, the present approach does not recourse to tensile strength as an influencing factor explicitly. This lack of consideration of tensile strength, which was already a feature of the originally proposed massivity index, ends up being somewhat compensated by the fact that the cracking risk is quantified within a range of massivity indexes, rather than on a deterministic value. It is also noted that tensile strength is sometimes harder to come by, or estimate, and it tends to lie within a relatively small range in typical massive concrete mixtures, hence further contributing to the reasoning of not being considered in this proposal

3.2.1. Relative heat correction factor, k_f

The first factor to be considered is that of the potential heat of hydration of the binder used. Currently, the massivity index does not consider the cement/binder type used or may implicitly assume that neat Portland cement - CEM I is used in all cases. Nonetheless, it is well recognised that binder type substantially

influences the rate and maximum heat generation. Although this can be a complicated task to incorporate from an engineering point of view, a correction factor for cement type may be applied to the massivity concept to allow for addition of blended cements. Such correction factor should offer a reduction on the calculated massivity and cracking proneness with use of cements other than CEM I. It is proposed that the factorised heat reduction when blended cements are used should occur relatively to a CEM I reference value. Therefore, this relative heat factor may be expressed as the ratio of heat output of blended cement with supplementary cementitious materials (SCMs) to that of neat Portland cement - CEM I. This pertains the assumption that the reduction in adiabatic temperature rise is roughly linear with the temperature rise, and so is the cracking proneness. Exemplar heat correction factor values have been calculated with semi-adiabatic data obtained from [38] for different cement types, considered typical in construction, as shown in Table 2. It is also recognised at this point that: a) the relative heat factor, k_f, may vary based on different calorimeter results and different cement types used and b) for very massive structures where near-adiabatic conditions are observed, heat evolved beyond 72 h during an adiabatic test might provide a more accurate indication of heat evolution to be used in calculating the relative heat correction factor. Such adaptation might also account for the observation that hydration of cementitious binders containing very high proportions of cement replacement materials is significantly decelerated, but, for the purposes of such study, the adapted approach is deemed adequate.

3.2.2. Binder content correction factor, k_b

Following the derivation of the relative heat correction factor, the significance of the total cementitious materials (binder) content may not be ignored. It has been well established that the binder content has a decisive influence on the potential temperature evolution within a section; the temperature effectively increases with binder content [39,40]. As a general quantification, it is accepted that cement hydration will generate a concrete temperature rise of approximately 4.7°C to 7.0°C per 50 kg of Portland cement per m^3 of concrete under adiabatic conditions [41,42], Under this context, assuming: a) an average temperature rise of 6.0°C per 50 kg of Portland cement and b) an average binder content of modern concrete in massive structures of 300 kg/m^3, a correction factor (k_b) based on binder content can be derived as the ratio of binder content in the mix to 300 kg/m^3, i.e. $k_b = \frac{\text{bindercontentin kg/m}^3}{300\text{kg/m}^3}$. Fig. 2 demonstrates how this factor may vary with binder content, also with relevance to temperature rise whilst the upper boundaries for all parameters have accounted for practicality and demonstrated experience, e.g. is not particularly common to get temperature rises of 70°C and above or binder content of 600 kg/m^3 and above, especially in massive concrete applications. Aiming simplicity, the variation of the correction factor k_b is linear, following also that the temperature rise under adiabatic conditions (e.g. in very massive concrete elements) is approximately linear. This implies that if the concrete is not under adiabatic conditions (e.g., in a thin element, thus more affected by environmental temperature), this correction factor yields even more conservative estimates, which is acceptable at this stage. It is, nevertheless, recognised that with the intention being to derive a code-like approach to the problem, the solution will be somewhat inherently imperfect. The relationship illustrated in Fig. 2 could be potentially extended for binder contents greater than 600 kg/m^3, e.g., for very high strength concrete applications, but it should be anticipated that the estimated adiabatic temperature rise is likely to constitute a significant overestimation of reality in these cases (more important as the element under analysis is thinner).

Table 2
Exemplar relative heat factors that can apply to massivity indexes depending on cementitious binder considered (heat evolution data from [38]).

Cement Type/ Combination	Heat evolved at 72 h [J/g] (Q), semi-adiabatic test	Relative heat factor $\left(k_f = \frac{Q_{SCM}}{Q_{CEMI}}\right)$
CEM I 42.5	366	1.00
CEM I 42.5 + 10% FA	325	0.89
CEM I 42.5 + 30% FA	200	0.55
CEM I 42.5 + 50% FA	112	0.31
CEM I 42.5 + 10% GGBS	334	0.91
CEM I 42.5 + 30% GGBS	255	0.70
CEM I 42.5 + 50% GGBS	232	0.63
CEM I 42.5 + 70% GGBS	157	0.43

3.2.3. Correction factor for temperature differential, $k_{\Delta T}$

The third and final massivity correction factor suggested and examined herein is representing the temperature differential in the member resulting from the interplay between fresh concrete temperature, peak concrete temperature and ambient temperature. This is aiming to account for the occurring temperature differential between core and surface and the herewith caused self-equilibrated stresses, respectively, the risk of surface cracking. This shall enable a targeted consideration of any measures of reducing the fresh concrete temperature at the time of placement below the average ambient temperature during curing as well as additional curing measures for thermal cracking mitigation due to the temperature differential.

Dealing with mass concrete, it will further be presumed that the core temperature will increase due to hydration according to adiabatic conditions, whereas the temperature at the surface is similar to the ambient temperature. It shall be noted that the assumption of adiabatic conditions in the interior is also in agreement with the rule of thumb for mass concrete according to [43,44], that a decrease of the fresh concrete temperature at the time of casting by 1°C decreases the peak concrete temperature in mass concrete by approximately 1°C. On the contrary, the assumption of a surface temperature similar to the ambient temperature is on the safe side and could be modified in case of targeted thermal curing measures. Nevertheless, defining the reference case with a fresh concrete temperature similar to the ambient temperature at the expected time of maximum temperature, the correction factor $k_{\Delta T}$ for any different case can basically be determined through:

$$k_{\Delta T} = \frac{T_{\text{fresh}} - T_{\text{ambient}} + T_{\text{adi,rise}}}{T_{\text{adi,rise}}} \quad (6)$$

where:

T_{fresh} – fresh concrete temperature;

$T_{\text{adi,rise}}$ – temperature increase due to hydration under adiabatic conditions (e.g., Fig. 2);

T_{ambient}– expected ambient temperature at time of maximum concrete temperature

It is recognised that for surface cracking to occur, the imposed strains (in this case the self-equilibrated thermal strains induced by T_{diff}) are dependent on the evolution of the elastic modulus, creep relaxation and the shape of eigen stresses according to the shape of the temperature distribution. From engineering perspective, however, these influencing factors are cancelled out by deriving the correction factor in relation to the reference case. It should be noted that since this is a pre-design approach and absence of temperature monitoring data on site is very much probable, expected average ambient temperatures at the anticipated time of placement can be obtained based on nearby weather stations and on climatological normal [45].

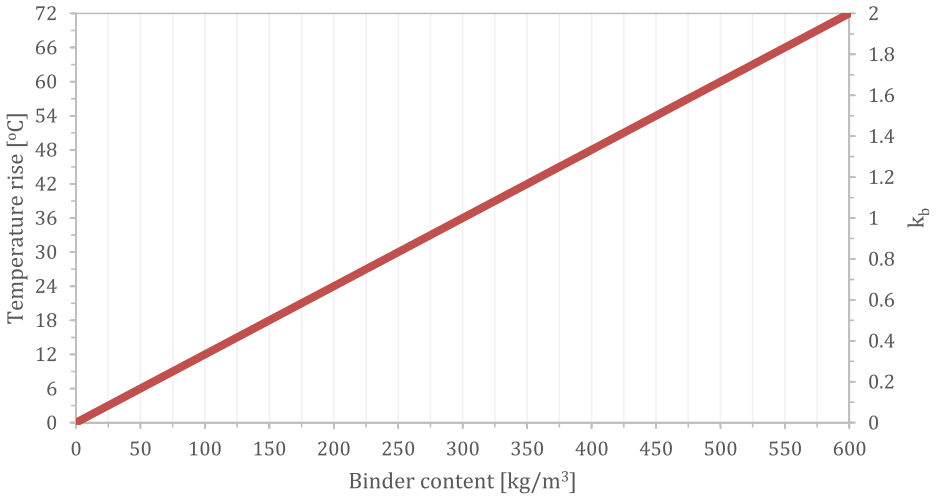

Fig. 2. Relationship between binder content and approximated temperature rise in concrete and k_b correction factor.

3.3. Validation of the enhanced massivity index

For validation purposes, the massivity concept by *Flaga* [37] (surface modulus approach) is enhanced using the above correction factors, i.e. the relative heat factor (k_f), binder content factor (k_b), and the temperature drop factor ($k_{\Delta T}$), as shown below in Table 3. As mentioned earlier, in this case, the surface modulus is divided by the product of the three factors whilst Flaga's limits for massive ($m_s \leq 2\text{m}^{-1}$) and semi-massive structures ($2\text{m}^{-1} < m_s < 15\text{m}^{-1}$) may be assumed to still apply. As all the case studies examined herein experienced cracking, few examples of uncracked massive concrete structures were collected from the literature and the correction factors were applied in their calculated surface modulus, i.e. enhanced massivity, in order to provide an additional preliminary validation of the updated massivity concept (also shown in Table 3).

The fact that in all the case studies SCMs were incorporated in the concrete, surface moduli, m_s, of the elements under investigation increased through the application of a correction factor for cementitious material's heat output, essentially decreasing the massivity of the structures containing SCMs after correction to a more semi-massive configuration. Nevertheless, the surface modulus of the investigated cases somewhat decreased with the application of the correction factor for binder content with the exception of the Itaipu dam, which was the only case in which the binder content was lower than the reference of 300 kg/m^3. The temperature differential factor, for the cases where the required information was known, further indicated an exacerbation in thermal cracking risk through decreasing the surface modulus with the exception of the Itaipu dam due to this structure's relatively low temperature development observed on site. Despite this increase in the surface modulus, the size of these structures is so substantial

Table 3
Application of the correction factors on the surface modulus of massive structures.

Structure type	Section No.	Dimensions [m]	m_s[m^{-1}] [62]	k_f	k_b	$k_{\Delta T}$	$\frac{m_s}{k_f * k_b * k_{\Delta T}}$[m^{-1}]
Massive blocks, rafts and footings	A.1.1.	5 × 5 × 4.6	1.02	0.70	1.47	N/A	0.84
	A.1.2.	1.8 × 1.8 × 1.8	2.78	0.70–0.43	1.08	N/A	3.07–5.95
		2.2 × 2.2 × 1.6	2.44	0.70–0.43	1.08	N/A	2.83–5.24
		2.2 × 2.2 × 2.2	2.27	0.70–0.43	1.08	N/A	2.52–4.87
		2.5 × 2.5 × 2.5	2.00	0.70–0.43	1.08	N/A	2.21–4.29
	A.1.3.	18.5 × 6.1 × 1.83	0.98	0.55	1.37	1.10*	1.17
		12.8 × 8.3 × 1.83	0.94	0.55	1.37	1.10*	1.12
		28.4 × 18.6 × 4.5	0.40	0.55	1.37	1.10*	0.47
		21.5 × 7.8 × 2.7	0.72	0.55	1.37	1.10*	0.86
		6.0 × 7.0 × 2.5	1.02	0.55	1.37	1.10*	1.23
Dams and spillways	A.2.1.	40 × 8 × 2.5	0.70	N/A	N/A	N/A	N/A
	A.2.2.	35 × 15 × 0.5 (lifts 1,2 & 3)	2.19	0.87	1.17	N/A	3.58
		35 × 15 × 2 (lifts 4,5,6)	0.69	0.87	1.17	N/A	1.01
		35 × 15 × 7.5 (whole structure)	0.32	0.87	1.17	N/A	0.39
	A.2.3.	17 × 36 × 85 (approx.)	0.25	0.89	0.40–0.66	0.37*	1.91–1.26
Massive columns and piers	A.3.1	3.5 (d) × 8	1.54	0.72	1.10	1.05	1.84
		3.5 (d) × 10	1.23	0.72	1.10	1.20	1.29
		4.5 (d) × 7.5	1.02	0.72	1.10	1.05	1.22
		4.5 (d) × 9	0.85	0.72	1.10	1.10	0.97
Examples of crack-free$^+$ structures of significant size							
Type	**Reference**	**Dimensions [m]**	$\boldsymbol{m_s}$**[m^{-1}]** [62]	$\boldsymbol{k_f}$	$\boldsymbol{k_b}$	$\boldsymbol{k_{\Delta T}}$	$\frac{m_s}{k_f * k_b * k_T * k_e}$[m^{-1}]
Massive walls	[46]	1.2 × 1.2 × 2.4	3.75	0.72	1.24	N/A	4.20
Massive walls	[46]	1.2 × 3.6 × 3.6	2.50	0.72	1.24	N/A	2.80
Wind turbine base	[47]	16.5 (d) × 2 (approx.)	0.93	0.55	1.08	1.07	1.46
Massive slab	[48]	143 × 41 × 0.35	2.91	1.00	0.95	1.20	2.55

*Average ambient temperature obtained from historical data

that the surface modulus remained below the upper limit of 2 m^{-1} indicating a significant risk for thermal cracking.

In general, the relative heat factor was apparently the most influential in the final values of surface moduli (or enhanced massivity) amidst the three derived correction factors. This is probably associated with the precautions for thermal cracking mitigation reflected in the variables in the other two factors not having been taken into consideration effectively during design. In any case, for the cracked structures, the combined factors $k_f \times k_b \times k_{\Delta T}$ were not able to increase the surface modulus above 2 m^{-1}, indicating that all of these cases would require further thermal cracking risk analysis. The exception was the case of the armour units in the Netherlands, where their surface modulus was exceeding 2 m^{-1} even before the application of the correction factors. This may slightly increase the ambiguity regarding the origin of the cracks in this case, as already mentioned in Section A.1.2 in relevance to thermal cracks and/or DEF/ASR cracks.

The three correction factors were also applied to the surface modulus of few uncracked massive concrete elements (where applicable). The uncracked cases considered were: (a) few massive walls (544 kg/m^3 binder content containing 15% fly ash) [46], (b) a wind turbine foundation (220 kg/m^3 of CEM II/A-L 42.5R and 105 kg/m^3 of fly ash) [47] and (c) a massive slab (285 kg/m^3 binder content with assumed CEM I cement used) [48]. For the majority of the examples, the calculated surface modulus was above the 2 m^{-1} limit for massive concrete structures; however, there was still an apparent influence of the factors in the enhanced massivity towards a decrease on thermal cracking proneness. Nevertheless, for the particular case of the uncracked wind turbine base in [47], the surface modulus increased considerably towards the limit for massive structure with the application of the three correction factors as it increased from 0.93 to 1.46 m^{-1} (an increase of 50%). It is believed that for this case in particular, the corrected surface modulus could have exceeded the upper limit if a less conservative relative heat factor would have been used (actual mix in this case contained a ternary binder), which is promising regarding the feasibility of these modifications. Moreover, for the case of the wind turbine foundation, the geometrical significance of such structure should prompt the designer to analyse thermal cracking proneness further, e.g., though FEM, regardless of the temperature control techniques employed.

Nevertheless, it is recognised that this enhanced massivity index is subject to further refinement to account for the effect of fresh concrete temperature and curing temperature on the heat generation which is also known to be different for concretes with SCMs [5,49–51] under non-adiabatic conditions and even for insulation characteristics, in order to incorporate the contributions of such influential factors, as well as to further validation considering cracked and uncracked massive concrete structures. Such initiative is covered by the future activities of the successor of RILEM TC 254-CMS (TC CCS: *Early-age and long-term crack width analysis in RC structures*).

3.4. Flowchart of processes for best practice

The processes involved with evaluating a potentially massive concrete structure in terms of the risk of thermal-related crack occurrence depend on several factors and may cause confusion to designers and contractors. While some massive (or mostly, semi-massive) concrete structures may be approached with simple/empirical solutions for thermal cracking mitigation, others require a more meticulous consideration of the influential phenomena, such as boundary conditions, heat of hydration or even shrinkage. The massivity concept may serve as a guiding element in determining the depth of analysis a structure might require for mitigating/controlling thermal cracks and provide an indication as to whether thermo-mechanical FEA should be considered, as depicted in the flowchart of Fig. 3. If a concrete element is not deemed massive enough, which corresponds to the right branch of the flowchart, then the designer can employ simple ready-to-use models to gain confidence with respect to thermal crack avoidance, e.g. models in the form of spreadsheets as those of CIRIA C766 [11]. It is not necessarily recommended that the engineer creates a 1D model himself to simulate structural behaviour as this can be as laborious as creating a finite element model. Instead, for simpler applications, already existing user-friendly spreadsheets may be employed, e.g. CIRIA C766 [11], Concrete Works [52] or suchlike.

It shall be the case, nevertheless, that the approach is agreed between the involved parties at early stages of the project, so that costs and sustainability of crack repair and crack avoidance/control (through FEM or mock-ups and monitoring) are compared; yet, experience dictates that the former is usually more cost demanding.

4. Summary and outlook

In this paper an investigation on massive concrete structures which experienced hardening-induced thermal cracking was conducted. The types of structures examined were massive foundation blocks and rafts, armour units, dams and spillways as well as massive columns as these types of structures are often impaired by thermal stresses. Based on the information gathered and analysis performed, the following conclusive remarks can be given:

- In the majority of the case studies, cracking probably occurred due to insufficient consideration of the associated relevant phenomena and boundary conditions whilst workmanship influences cannot be ruled out. Nevertheless, collaboration between the involved parties, e.g. designers, contractors and/or concrete producers, at early stages of the project becomes an important factor in deciding best approach for controlling defects due to thermal cracking. In many cases, crack repair could be more expensive than adequately designing a structure for thermal crack control or than applying temperature control techniques (pre-/post-cooling).
- In the analysed cases finite element analysis (FEA) was used as a tool for forensic engineering purposes. However, such analysis usually comprises of the same techniques as pre-analysing the structure for cracking. It is, therefore, recommended that FEA is undertaken in all relevant cases as part of the design. As such, indications for the necessity of pre/post-cooling techniques or alterations in mix design and curing methods will be given. Moreover, that allows to predict stresses and design appropriate reinforcement as in some cases insufficient reinforcement was found to be the reason of extensive cracking.
- The concept of massivity can be potentially used to indicate whether a concrete structure will be susceptible to hardening-induced cracking caused by internal restraint of thermal strains (considering that external restraint is near-negligible in massive concrete applications) and consequently, whether more advanced approaches, such as numerical simulations, would be required for mitigating associated defects. One of the primary aims of this study was to enhance the application of the massivity indexes. The modified surface modulus was recommended as a geometrical measure of massivity and thermal cracking risk in which correction factors were derived and proposed to account for cumulative hydration heat depending on the type of the binder, binder content and influence of ambient temperature and temperature differentials. It was demon-

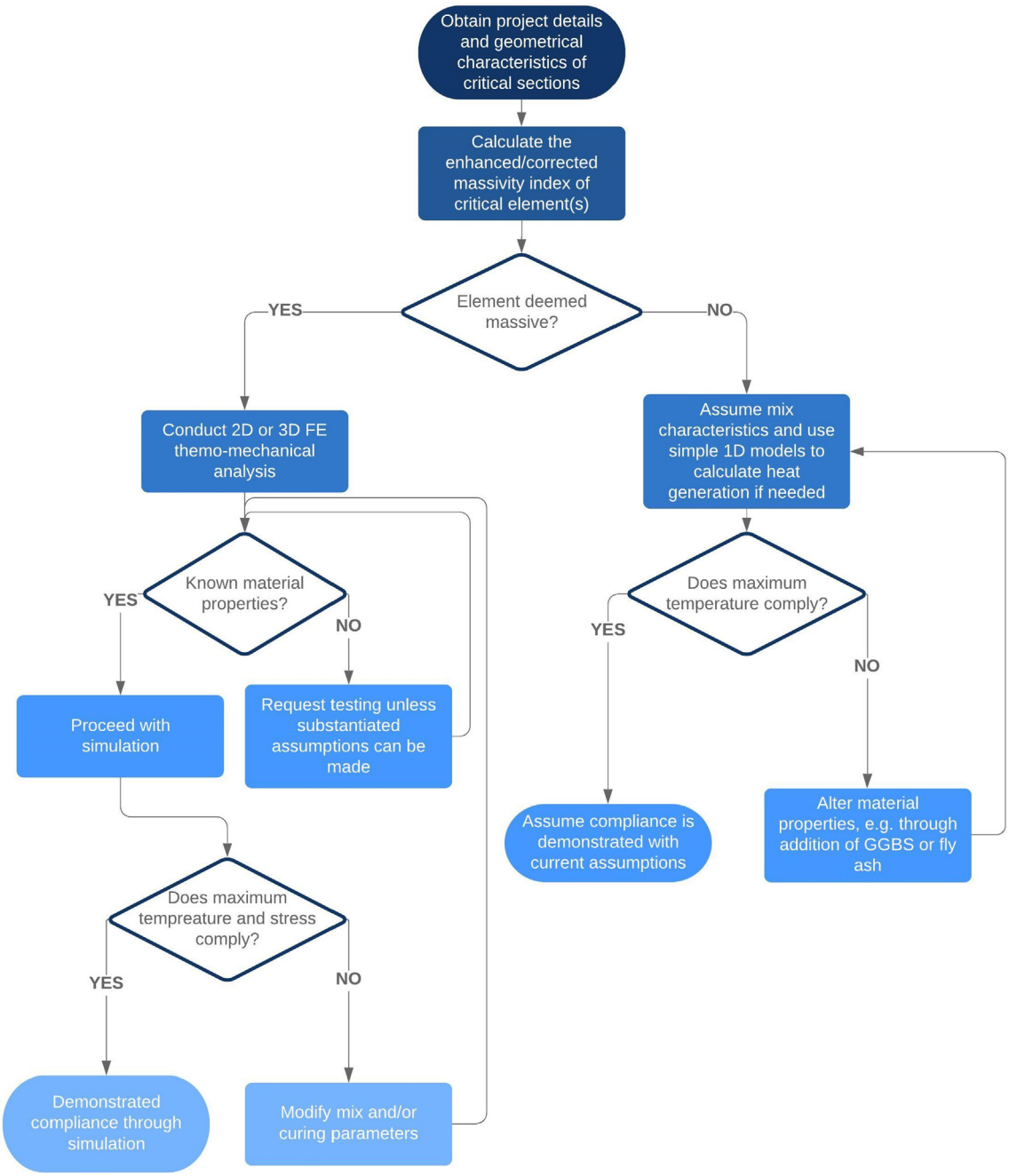

Fig. 3. Flowchart with recommended processes involved for assessing the risk of thermal cracking of massive and semi-massive structures.

strated that the enhanced massivity index proposed can provide designers and contractors with a more robust pre-design assessment of likelihood of thermal cracking occurrence. Nevertheless, they are subject to further refinement and validation. As a next step, it would be helpful to conduct numerical analysis to further improve the validity of the factors for a range of structures and boundary conditions.

- In addition to FEM, construction of mock-ups and derivation of monitoring programmes are also recommended, in applications with high cracking risk, as they will further increase confidence on the validity of the decided approach.

This study focused on quantifying the likelihood of crack in massive concrete structures due to self-equilibrated temperature differentials and stresses which may result in surface cracking. Work is continuing within RILEM TC CCS, the successor of TC 254-CMS, to quantify the risk of through cracking or bending cracking from the presence of external restraint which is relevant to thinner, than those investigated, elements and require assessment of the restraining condition with regard to the types of members involved.

CRediT authorship contribution statement

Fragkoulis Kanavaris: Conceptualization, Formal analysis, Resources, Writing - original draft, Writing - review & editing. **Agnieszka Jędrzejewska:** Conceptualization, Writing - original draft, Writing - review & editing. **Ioannis P. Sfikas:** Writing - review & editing. **Dirk Schlicke:** Conceptualization, Writing - orig-

inal draft, Writing - review & editing. **Selmo Kuperman:** Resources. **Vít Šmilauer:** Conceptualization, Resources, Writing - original draft, Writing - review & editing. **Túlio Honório:** Resources, Writing - review & editing. **Eduardo M.R. Fairbairn:** Resources, Writing - review & editing. **Gabriella Valentim:** Resources. **Etore Funchal Faria:** Resources. **Miguel Azenha:** Conceptualization, Writing - review & editing.

Declaration of Competing Interest

The authors declare that they have no known competing financial interests or personal relationships that could have appeared to influence the work reported in this paper.

Acknowledgements

This study is an output of the Working Group 7 of the RILEM TC 254-CMS: Thermal cracking in massive concrete structures (Chair: Eduardo Fairbairn, Secretary: Miguel Azenha) which has now been succeeded by RILEM TC CCS: Early-age and long-term crack width analysis in RC structures (Chair: Miguel Azenha, Deputy Chair: Fragkoulis Kanavaris). The authors are grateful to all members of the technical committees for the helpful discussions held and insightful comments/suggestions given for this document with particular gratitude given to Dr Carlos Serra.

In the particular case of the author from the Silesian University of Technology funding of the research by the Polish Ministry of Science and Higher Education within the grant BK-298/RB6/2020 is acknowledged.

Funding provided by the Portuguese Foundation for Science and Technology (FCT) to the Research Project IntegraCrete PTDC/ECM-EST/1056/2014 (POCI-01-0145-FEDER-016841), as well to the Research Unit ISISE (POCI-01-0145-FEDER-007633) is gratefully acknowledged. The support of COST Action TU1404 in the networking actions necessary for this work is also acknowledged.

The authors from COPPE/UFRJ acknowledge the Brazilian agencies CAPES – Finance Code 001, CNPq and FAPÈRJ for partial funding of the present research. They are also grateful to ITAIPU Binacional for providing information about Itaipu dam.

The author from Czech Technical University in Prague acknowledge data sharing from Červenka consulting and Škoda Praha Invest. The Czech Science Foundation is acknowledged for supporting creep and shrinkage model calibration within the project 19-20666S.

The contents of this paper reflect the views of the authors, who are responsible for the validity and accuracy of presented data, and do not necessarily reflect the views of their affiliated organisations.

Appendix

A number of representative case studies from the literature, elaborated by own experience/involvement from the authors, are presented and discussed in this section for a range of typical massive concrete structures.

A.1. Massive blocks, rafts and footings

A.1.1. Massive abutment block in Czech Republic

Surface cracking occurred in a massive abutment/anchorage block in Czech Republic, approximately one year after casting. The block measured 5 × 5 × 4.57 m (length × width × height) and was cast in summer 2009. The concrete strength class was C35/45 with an exposure class XC1. The concrete composed of a binder, *b*, incorporating 400 kg/m^3 of a low-strength slag-based cement, CEM II/B-S 32.5 R (21–35% of ground granulated blast-furnace slag), and 40 kg/m^3 of fly ash, resulting in a low-heat ternary blend, 175 kg/m^3 of water, *w* (w/b of 0.4), 1809 kg/m^3 of combined fine and coarse aggregates and 7 kg/m^3 of admixtures (3 kg of plasticiser and 4 kg of superplasticiser).

The massive block was vertically reinforced with three layers of bars with a diameter of 32 mm located up to 500 mm away from the external surface. With a total of 248 rebars, as shown in Fig. A.1a,b, the vertical reinforcement ratio was 0.8%. Horizontally, 10 and 12 mm diameter stirrups were installed in two layers, with a vertical spacing of 200 mm, resulting in a reinforcement ratio in the longitudinal direction of only 0.019%.

After approximately 1 year from concrete casting, vertical cracks with a width ranging from 0.1 to 0.5 mm were detected, as shown in Fig. A.1c,d. Some 600 mm deep core samples revealed that the cracks were running into the block surpassing reinforcement layers. The assumption at the time was that the crack likely runs through the block, although this was never experimentally confirmed. A thermo-mechanical simulation has confirmed that the cause of cracking was excessive hydration heat and the observed crack widths are compliant with the small amounts of horizontal reinforcement [53].

A blind, *a-posteriori* simulation in the same study resulted in a temperature rise prediction from a starting temperature of 20°C to a maximum of 61°C at 9 days, see Fig. A.2a, whilst the block cooled down to ambient temperature after approximately 100 days.

The thermo-mechanical analysis using finite elements accounted for concrete creep and shrinkage, as well as fracture mechanics. The literature model used for creep and shrinkage [54,55] takes into account temperature strains and autogenous shrinkage, while it neglects drying shrinkage due to the massive size of the element. It was calculated that the average predicted crack width was approximately 0.23 mm which falls within the range of measured crack widths on the concrete surface (0.1–0.5 mm), see Fig. A.2b. It is recognised, however, that including drying shrinkage in the simulation would have resulted in increased predicted surface crack widths, even by 0.3 mm.

After 720 days, when the cracks had fully developed, the columns supported by the massive anchorage/abutment block were loaded in the model up to 100% of the design load and then loaded further up to failure in order to evaluate their ultimate strength. It is noted that the block was designed for axial force of 168 MN, reaction moments up to 25 MNm and horizontal forces up to 6.2 MN. The analysis confirmed that the columns had a sufficient load-carrying capacity, i.e. the overloading factor was approximately 2, as compared to a global safety factor of 1.27 in accordance with EN 1992-1-1 [56]. However, due to the initial cracking, the block strength and loading capacity were reported by the same study to have been reduced by almost 30%. Insufficient horizontal reinforcement, as compared to minimum reinforcement requirements, could not contribute to the mitigation of vertical cracking. The blocks were later post-tensioned, in order to compensate for the missing horizontal reinforcement.

A detailed thermo-mechanical analysis on a similar structure in the same study revealed that minimum vertical reinforcement ratio effective in preventing crack localization into a few splitting macrocracks is 0.3% when reinforcement is more concentrated around perimeter than in the core (all vertical steel is divided to total cross section concrete area). A reinforcement ratio of 0.4% was able to keep crack under 0.25 mm width both at surface and core. However, the actual reinforcement ratio was much lower than what was required, leading to insufficient crack control.

A.1.2. Concrete armour unit in Ijmuiden, the Netherlands

Significant damage and excessive cracking on four massive (unreinforced) concrete armour units was observed in the Ijmuiden breakwaters in the Netherlands, see Fig. A.3 [57,58].

The armour units varied on dimensions and weight, i.e. 1.8 × 1.8 × 1.8 m, 2.2 × 2.2 × 1.6 m, 2.2 × 2.2 × 2.2 m and 2.5 × 2.5 × 2.

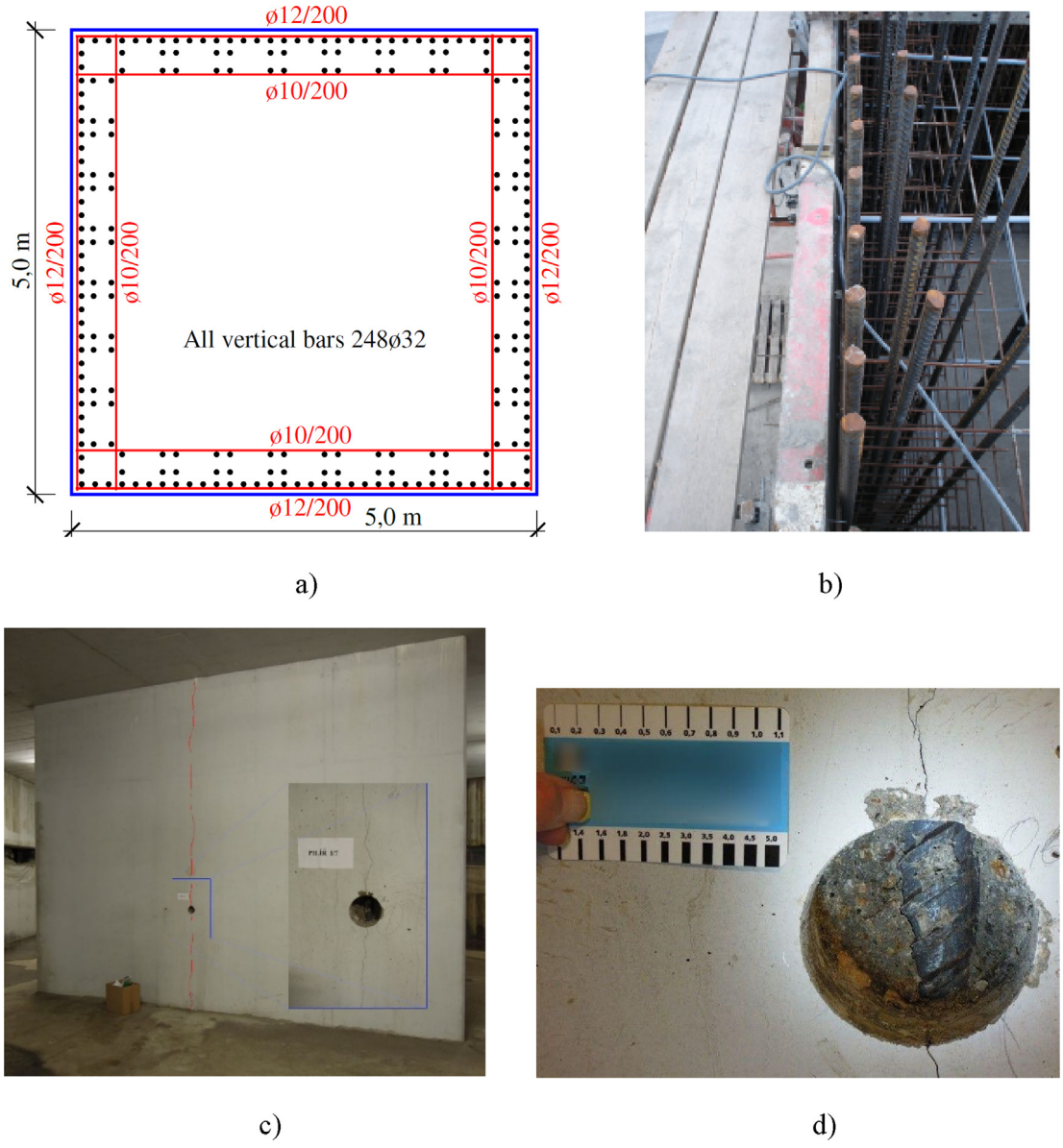

Fig. A.1. a) reinforcement of the massive abutment block, b) detail of reinforced surface area, note sub-marginal horizontal reinforcement in the block, c) cracked block after 1 year with vertical macro-cracks, d) detailed view of a drilled core through a 0.4 mm wide vertical crack (Courtesy of ČEZ, a.s).

5 m and 17, 22, 30 and 45 tonnes respectively. Their construction took place between 1972 and 1987 whilst further blocks were added in 1995. The composition of the concrete used included cement replacement with GGBS at a percentage of 30 but mostly 70%, whilst the binder content varied between approximately 300 and 350 kg/m^3. It should be noted that the mix used had higher than normal density of about 2800 kg/m^3.

The wooden formwork was removed at 1 day after casting and transportation of the units commenced at 3 days after casting whilst it was suggested that the selection of timber forms contributed to twice as high cracking risk when compared to the use of steel formwork [35,36]. Defects and cracks of different patterns were observed at various locations and included circular, vertical and horizontal cracks on the concrete surfaces, as well as dislodging of pieces of concrete. Orthogonal cracks were predominately observed on the upper side of the elements due to this surface being directly exposed to variations of environmental conditions and subjected to potentially poorer compaction whilst the white efflorescence emerging from the cracks was probably related to the reaction between free lime and sea water. Based on the analysis performed in [57,58], it was suggested that the cracks were formed mainly due to thermal stresses caused by internal restraint and have probably initiated from the core towards the surface of the unit once the concrete had cooled down to ambient temperature at an age of 28 days after casting (Fig. A.3). It is worth noting that a similar study on deteriorated armour units in the UK [59] has shown that thermal stresses were not critical and has identified alkali-silica reaction (ASR) as the main cause of deterioration and cracking.

A.1.3. Massive concrete footings on bridges in the USA

An intensive inspection schedule described in [60,61] revealed excessive cracking in massive concrete bridge footings in coastal environments in North Carolina (NC), USA. Bridges inspected included the Oak Island Bridge (OIB), the Sunset Beach Bridge (SBB) and the US 17 Wilmington Bypass Bridge (WBB). The inspections were conducted approximately 3, 3, and 9 years after the con-

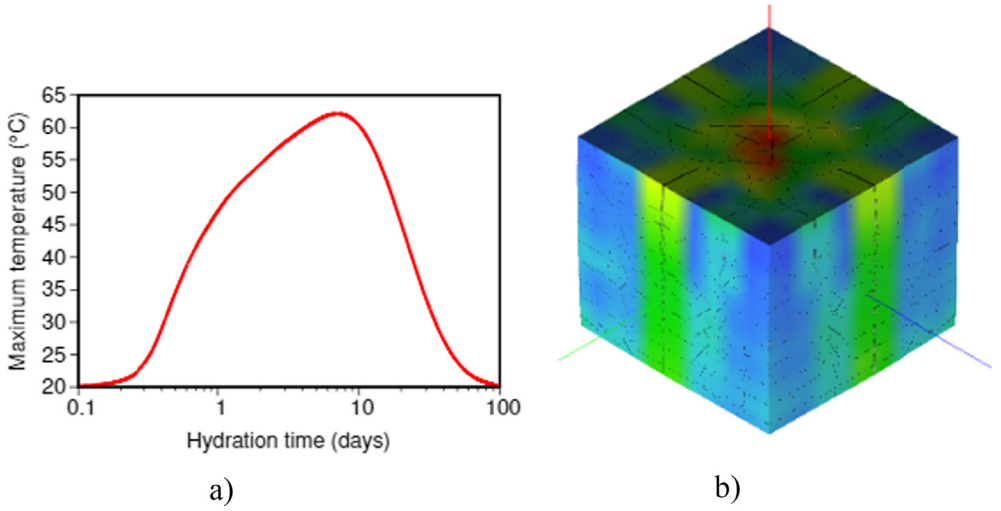

Fig. A.2. Simulation of the foundation block: a) temperature evolution in the core and b) crack state at 720 days after casting [31].

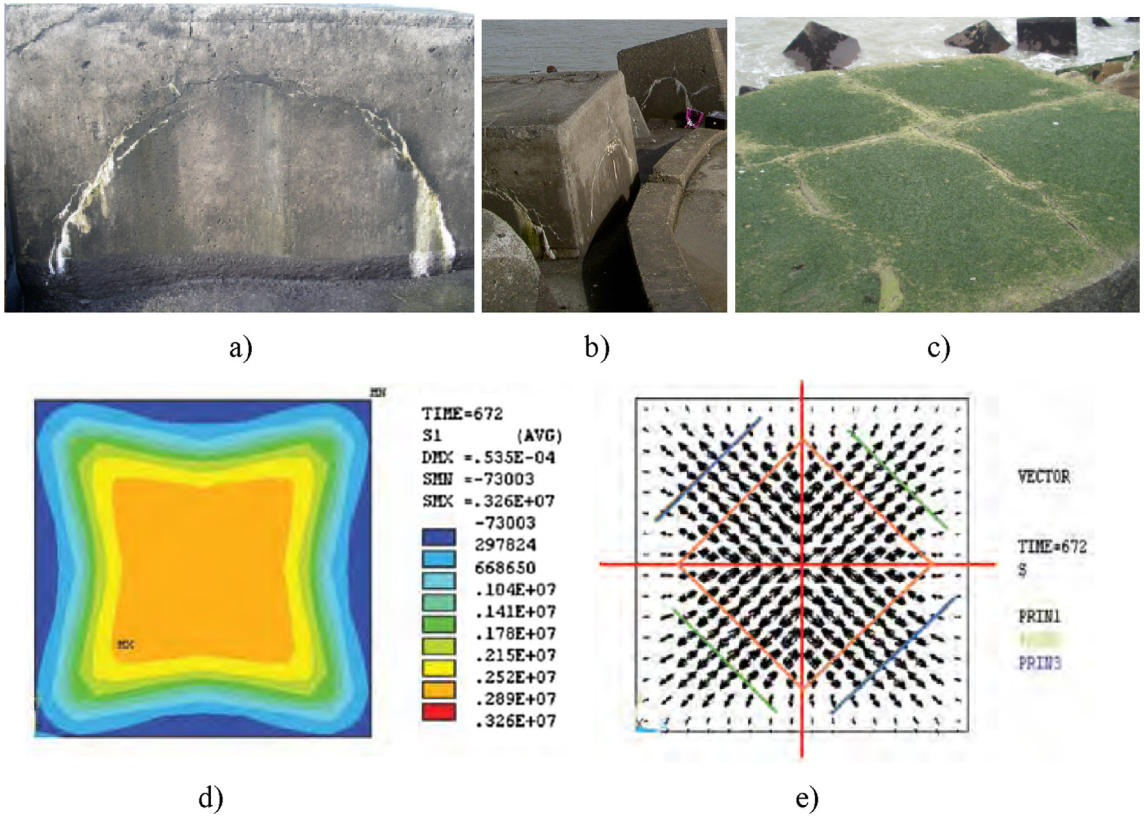

Fig. A.3. a-c) Examples of cracking observed in the mass concrete armour units in Ijmuiden and d, e) numerical simulation of residual stresses and cracking after 672 days [57,58].

struction of the footing of OIB, SBB and WBB, respectively, with the main aim being the assessment of the structural condition and cracking occurrence.

The bridge footings were designed accounting also for thermal control plans according to North Carolina Department of Transportation (NCDOT) recommendations, e.g. take special provisions for concrete masses above 1.5 m^3, limit temperature differential between concrete surface and concrete to 19.4°C, limit maximum fresh concrete temperature to 23.9°C. Similar requirements are found in ACI 301–10 [62], however, NCDOT further limits binder content to 410 kg/m^3 and suggests temperature monitoring. Material properties and recorded temperature were made available to complement the inspections findings, as shown in Table A.1. In most of the occasions, additional thermal control measures were taken during construction, such as the application of thermal blankets and use of steel formwork which was left in place for up to 1 or 2 weeks. However, regardless of these measures, excessive cracking did occur in both the vertical and horizontal directions and in the case of WBB map cracking was also reported. Crack repairs were realised before the time of the inspections, however, there were still: a) unrepaired cracks present and b) repaired cracks re-opened.

Table A.1
Information associated with cracked bridge footings in [60,61].

Parameter	Structure's footings investigated		
	OIB	SBB	WBB
Dimensions [m]	18.5 × 6.1 × 1.83	12.8 × 8.3 × 1.83	28.4 × 18.6 × 4.521.5 × 7.8 × 2.76.0 × 7.0 × 2.5
Binder composition	65% CEM I, 30% FA, 5% SF	65% CEM I, 30% FA, 5% SF	75% CEM I, 25% FA
Total binder content [kg/m^3]	410	410	410
Water-to-binder ratio, w/b	0.34	0.32	0.34
Air content	6%	6%	6%
Design / Delivered 28-day cylinder strength [MPa]	34 / 42	34 / 41	34 / 41
Placing temperature [°C]	20	18	20
Maximum concrete temperature [°C]	71	–	–
Time at which max temperature was developed [hours]	40	–	–
Maximum temperature differential [°C]	23	–	–
Time at which maximum temperature differential was developed [hours]	84	–	–
Crack widths [mm]	0.12–0.25	0.25–0.63	–

A forensic investigation involving viscoelastic thermo-mechanical FE analysis is also presented in the referenced studies, with the main aim being the calculation of the thermal cracking index, i.e. the ratio of tensile strength to tensile stress, at various time instances, i.e. see Fig. A.4. As temperature monitoring were only available for OIB, the indication of maximum temperature rise and differential was relying on the FEA results, which are shown in Table A.2. It was demonstrated that the likelihood of cracking was relatively high for all footings investigated, but most notably for WBB, which also experienced the most intensive cracking compared to OIB and SBB, since the calculated temperature differential exceeded 50°C. This was attributed to the size of the footing and to early formwork removal whilst, it was shown that from a mix design perspective, solely a 25–30% fly ash as a replacement might not have been adequate for controlling the hydration to a satisfactory extent so that thermal cracking is mitigated.

A.2. Concrete dams and spillways

A.2.1. Concrete buttress dam in Sweden

Extensive cracking was observed in a massive concrete buttress dam at Storfinnforsen, a major hydropower dam in northern Sweden, as reported in [63,64]. Buttress dams consist of tall concrete monoliths, each with a front-plate facing the water and supported by buttresses, as shown in Fig. A.5. The Storfinnforsen hydropower buttress dam consisted of some 100 monoliths with an approximate maximum height of 40 m, 8 m wide front-plates with 2.5 m base thickness and 1–1.5 m crest thickness. Two layers of Ø18 rebars were placed in the vertical and horizontal direction every 400 mm through the monoliths, whilst the concrete cover to reinforcement was 50 mm. More detailed information regarding mix composition was not made available. The total length of the dam was approximately 1.2 km and its construction was completed in 1954.

Upon completion of construction, horizontal cracks were detected in the lower part of the front-plates which led to water leakage from the reservoir. The cracks, which most possibly occurred during the concrete cooling phase due to thermal stresses from high maximum temperatures and profound thermal shock effect [65], were categorised in four different types (not to be confused with fracture mechanics' mode of crack propagation) as shown in Fig. A.5: 1) horizontal cracks on both faces of the front-plates, 2) inclined cracks initiating from the front-plate and extending towards the foundation through the buttress, 3) inclined cracks that had propagated from the internal passage of inspection and 4) vertical cracks emerging from the foundation.

In an inspection of the condition of the dam publicised in 1991, it was noted that type 1 and 2 cracks were observed prior to the scheduled installation of an insulating wall (for ice-growth prevention and supply of heated air from the underground power station), whilst type 3 and 4 cracks appeared few years after the installation of the wall. Further analysis of the structural behaviour of the dam in [63] indicated that cracking has most likely occurred due to seasonal temperature variation with type 1 cracks occurring during summer and type 2 cracks during winter. Surprisingly enough, the insulating wall installed in the dam at a later instant was claimed as responsible for causing type 3 and 4 cracks which appeared during winter seasons due to the restrained contraction of concrete.

In this case, a non-linear finite element model was created as described in [63], and it was shown that apart from the internal restraining conditions resulting from the massive geometry of the dam, the external restraint of concrete's volumetric changes was also significant and led to generation of high tensile stresses and was deemed responsible for type 4 cracks. In addition, the condition of the thermally-induced cracks at early ages was exacerbated or even new cracks were formed from volumetric changes due to seasonal temperature variation, whilst it was shown that it may even take years for a stabilised cracking pattern to be maintained.

A.2.2. Hydropower plant spillway in South America

Numerous cracks appeared on the lateral surface of a spillway block of a relatively small hydropower plant in South America during its construction, as described in [66].

The dimensions of the spillway block were 35 × 15 m, cast in three lifts of 0.5 m and three of 2 m cast a day each, with a resultant total height of 7.5 m. The concrete mix contained 350 kg/m^3 of an equivalent to the EN 197 CEM II/A cement with a w/c of 0.52. The ambient temperature during placement was approximately 32°C, very much near the upper limit set by guidance documents on hot weather concreting, such as [67,68]. It is worth noting that no instrumentation/monitoring programme was implemented during construction and no pre-cooling or post-cooling measures were taken.

The resultant vertical cracks, see Fig. A.6, immediately raised concerns with respect to the integrity and serviceability of the spillway, as they were of considerable width, ranging from 0.2 to 1.2 mm. To assess the significance of the lateral cracks, water under pressure was injected only to ultimately demonstrate that the cracks were propagating through the whole section thickness. The cracks were repaired using epoxy grout.

A forensic investigation using numerical simulations revealed that the formation of the cracks was due to generated thermal stresses in the spillway block. It was computed through FEA that temperatures up to 62.5°C were reached within the core of the block, while the thermal shock from formwork striking at 3 days

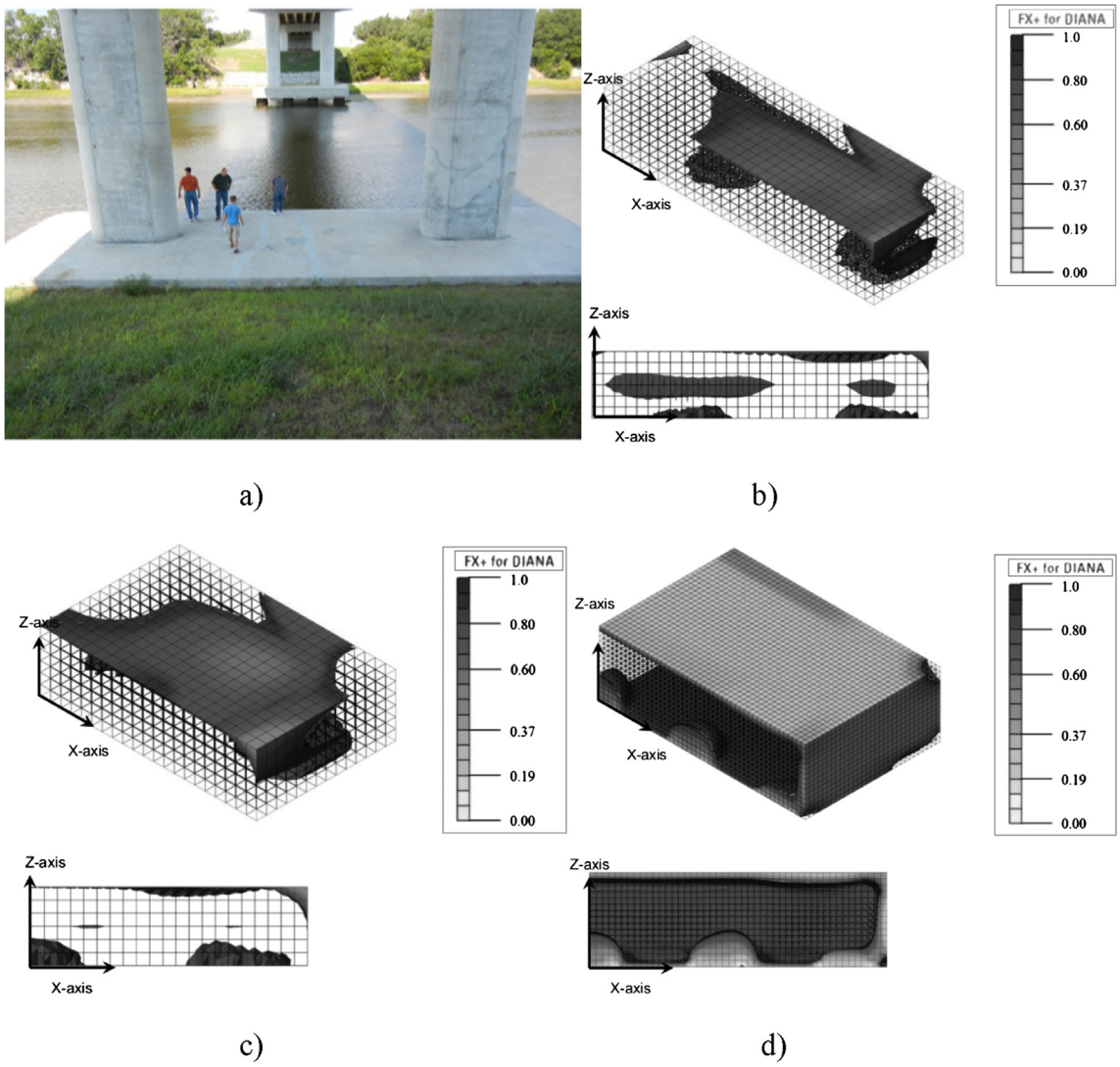

Fig. A.4. a) View of IOB footing. Some repaired cracks are visible at the middle of the footing, b) IOB footing FEA cracking index at 116 h after casting, c) SBB footing FEA cracking index at 86 h after casting and d) WBB footing FEA cracking index at 156 h after casting [60,61] (reprinted with permission of ASCE).

Table A.2
Thermal results from simulations in [60,61].

Simulation result	Structure's footings investigated		
	OIB	SBB	WBB
Maximum concrete temperature [°C]	71	67	78
Time at which max temperature was developed [hours]	40	51	120
Maximum temperature differential [°C]	25	21	55
Time at which maximum temperature differential was developed [hours]	116	86	156

contributed to temperature differentials as high as 42°C. It was estimated that cracks could have initiated from 10 to 100 days after casting due to the increased size of the structure.

A.2.3. Itaipu hydropower plant and buttress dam in Brazil/Paraguay

Itaipu hydroelectric power plant is the largest producer of electric energy in the world, it has produced around 100 MWh of annual generation and 2.5 billion of MWh since it started operating [69]. The Itaipu dam is composed of structures made of concrete (about 13,000,000 m^3), rock and earthfill that serve to harness the water and obtain the difference in levels of 120 m, which allows the operation of the turbines. The buttress dam constitutes the right bank dam, and the connection dams on the left and right sides of the main dam. In total, there are 83 buttress blocks with 17 m of width and height varying from 35 m to 85 m, see Fig. A.7. The upstream face has a slope of 0.58H: 1.00 V and the downstream face side of 0.46H: 1.00 V [48].

The construction of the first buttresses blocks, which were located in the right bank dam, was initiated in November 1978. The design fresh concrete temperature was 7°C. In order to obtain such fresh concrete temperature, some pre-cooling measures were taken, such as cooling of coarse aggregates, by aspersion on belt and cool air supply and replacing part of the mixture water with ice. The average temperature achieved at batch plants was 6°C [71] whilst the maximum temperatures reached in the core of the blocks were 36°C in the head and 34°C in the buttress at 90 days. It should be noted that it took about 4 to 5 years for temperature equalisation to occur [70].

The first cracks were noticed by visual inspection in August 1980 [72]. There were cracks in 34 of the 47 blocks built beyond El. 190 m in the right bank dam, which were located mainly in the buttress, and sometimes in the head of the blocks. The cracks

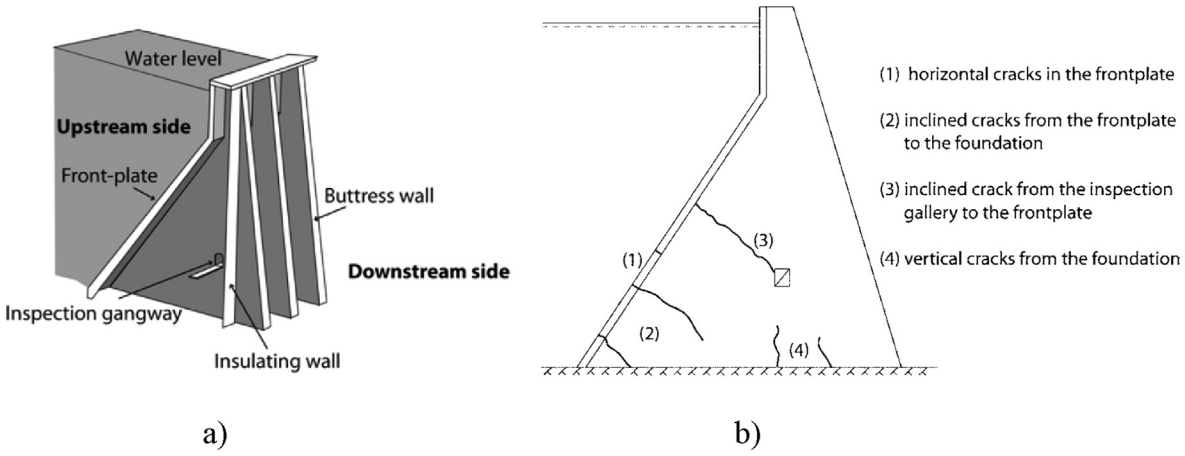

Fig. A.5. a) Buttress dam layout and b) cracking observed on-site of the Storfinnforsen hydropower dam [63,64].

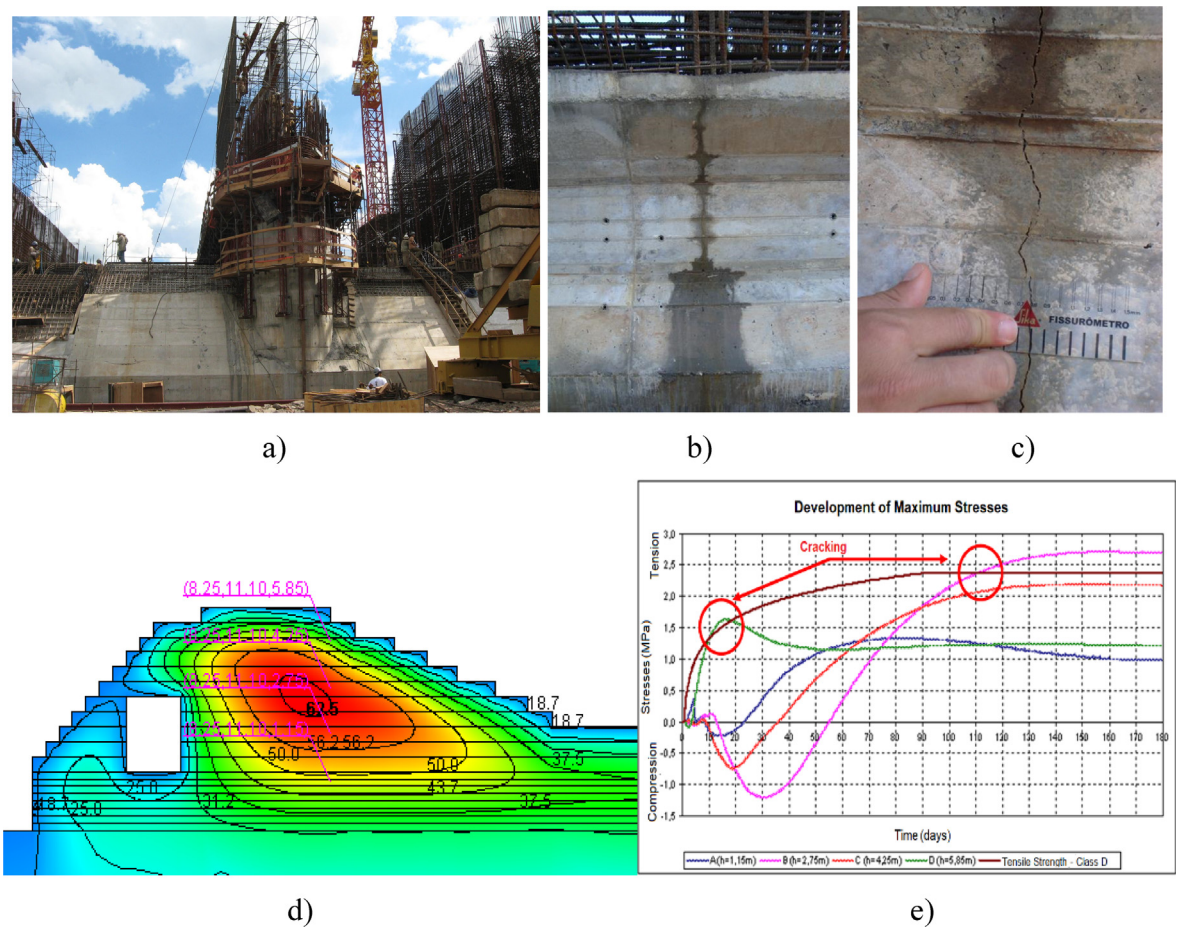

Fig. A.6. a) View of the spillway under construction, b, c) resultant thermal cracks and d, e) results from numerical simulations (bottom) [66].

were vertical, began on the foundation and were located at the upstream or at the downstream thirds of the base [72]. They were shallow, had an opening varying between 0.3 and 0.9 mm and the most significant ones were 10 m to 20 m long, as shown in Fig. A.7 [72,23].

The assessment of the concrete was made by Itaipu Laboratory, where technological studies took place, such as adiabatic temperature rise, thermal properties, tensile strength, creep, autogenous shrinkage and tensile strain capacity [71]. This extensive laboratory investigation in combination with the traditionally considerable experience of Brazil in dam construction was used to determine the mix design of the concretes. For the buttresses dams, there were two types of concrete used to build the first blocks. The first type, used for the first 6 layers, had a cement content of 169 kg/m^3, fly-ash content of 20 kg/m^3 and water content of 108 kg/m^3, which gave a w/b of 0.54. The maximum aggregate diameter of this concrete was 76 mm and the design compressive strength was 21 MPa at 360 days. The second type had a Portland

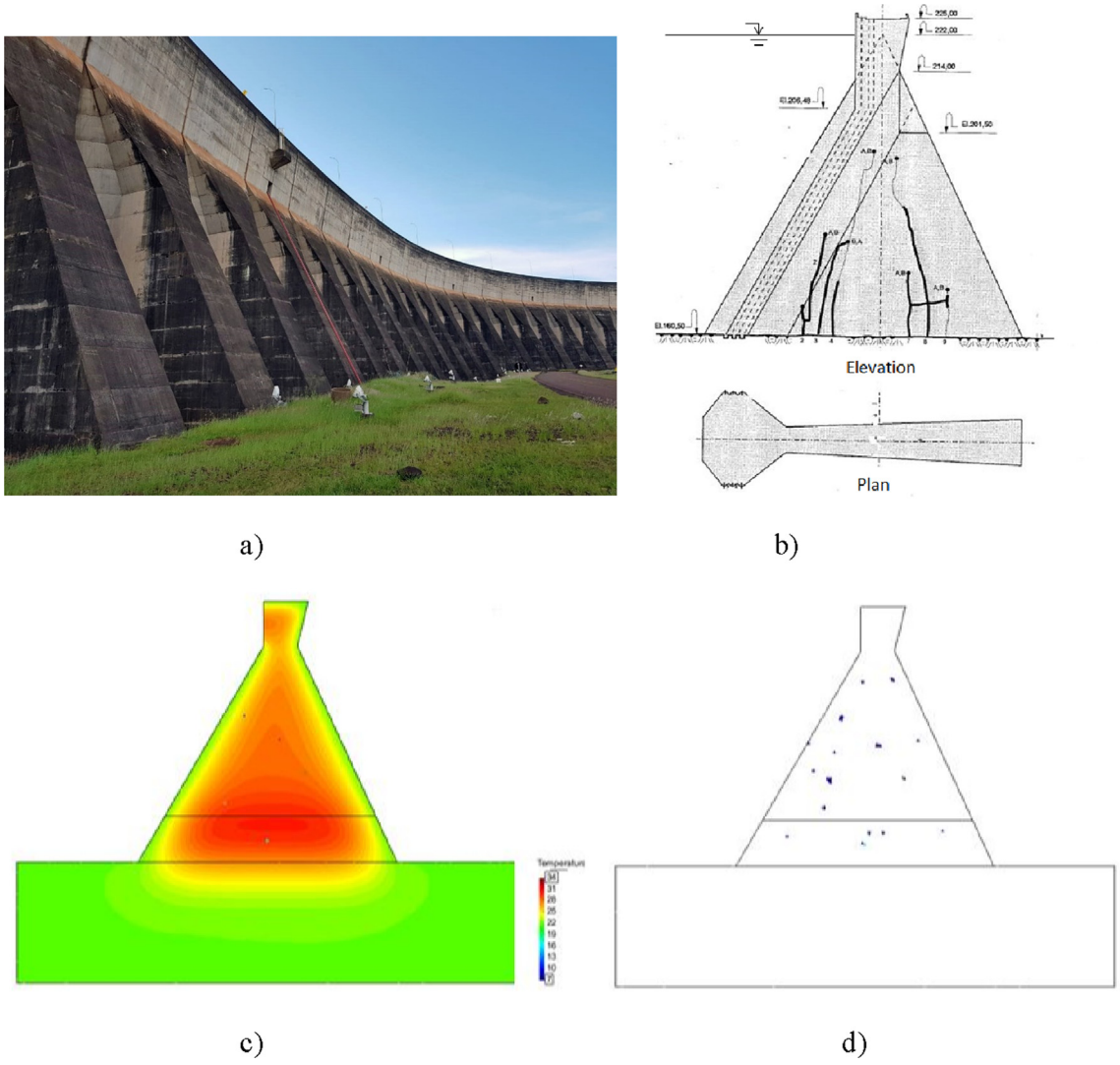

Fig. A.7. a) Typical buttress block [72,23], b) crack schematic of the buttress block [50,23], c) temperature distribution results from FEA at 365 days after casting [73] and d) cracking index (tensile stress / tensile strength) greater than 1 at 365 days after casting [73].

cement content of 108 kg/m^3, fly ash content of 13 kg/m^3 and water content of 85 kg/m^3, which gave a w/b of 0.67. The maximum aggregate diameter of this second type of concrete was 152 mm and its design compressive strength was 14 MPa at 360 days [71].

A performance evaluation and control programme were developed and conducted in parallel with the construction of the dam, which included mapping, extraction of cores and other monitoring tests [72]. These cracks were repaired using epoxy material and some measures were taken to prevent the formation of new cracks, such as: addition of a contraction joint parallel to the upstream face between the head and the buttress, adoption of a smaller cement content in concrete used in the first layers, modification of the pour sizes of first 3 layers, incorporation of a different steel mesh type. These measures appeared to be sufficient to keep cracks stabilised, and safety and durability of the structures were considered to be ensured.

A 2D simplified FEM analysis conducted with computer code DAMTHE [74,75] which uses a thermo-chemo-mechanical model was carried out for a typical block. Fig. A.7c and 7d show the temperature fields and regions with cracking indexes greater than 1 for 365 days after casting. The analysis resulted in a maximum temperature of 33°C in the core and 22°C in the surface at 85 days whilst in the simulation the cracks were noticed at 38 days. The cracking indexes (tensile stress/tensile strength as a function of degree of hydration) calculated confirm the tendency for thermal cracking with a pattern similar to the one verified in the field [73].

A.3. Massive columns and piers

A.3.1. Massive concrete piers under a viaduct in Italy

Another case of significant damage from thermal effects is that of several massive concrete columns/piers in a viaduct in Italy, as reported in [76].

The piers supporting the viaduct have a varying height of 7.50 to 10 m, a diameter of either 3.5 or 4.5 m and are sitting on 2 m (average) thick foundations. It should be noted that a few of the 3.5-m diameter piers were designed as hollow, yet the majority of them are solid. The concrete mix used had 0.43 w/c ratio and contained 330 kg/m^3 CEM IV/A, as a measure to reduce the heat of hydration. Concrete was cast during low-temperature months whilst the formwork was removed 1 day after casting. Information regarding casting time, removal of formwork, casting temperature and crack appearance is shown in Table A.3. After the first few days from formwork removal cracking was observed on a considerable number of piers in both vertical and horizontal directions, with a crack width varying from 0.05 to 0.3 mm as shown in Fig. A.8.

Table A.3
Information associated with cracked bridge solid piers in [54] (NR: Not reported).

Diameter [m]	Days (after casting)		Temperature [°C]	
	Formwork removal	Crack reporting	Ambient	Concrete at casting
3.5	1	1	14	14
3.5	2	5	NR	NR
4.5	2	5	16	18
4.5	3	7	NR	NR
3.5	2	10	20	22
3.5	2	5	4	12
4.5	2	6	8	12

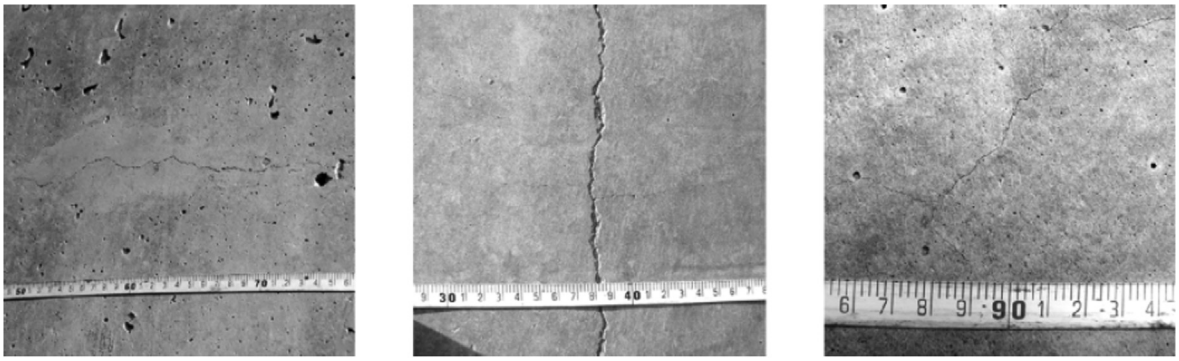

Fig. A.8. Typical cracks in the piers: a) horizontal, b) vertical and c) randomly orientated [54].

The size of the elements dictated the need of precautions to be taken to mitigate the thermal cracking risk. Although a lower heat of hydration cement (268 kJ/kg) was considered compared to CEM I, this proved to be insufficient for mitigating thermal cracking. Further analysis revealed that temperatures in the core of the solid piers would have probably reached 65°C, yielding significant thermal gradients that were deemed to be responsible for cracking. Further measures should have been taken to enhance the thermal cracking resistance of the piers, as described in [54], such as consideration of construction stages, insulated formwork kept for several days, incorporating a cooling pipe system in the piers (a rather not so viable option) or hollow piers instead of predominantly solid ones. Nonetheless, with respect to the former, there was no clarification as to whether the hollow piers experienced less cracking, but it can be naturally assumed that they would have experienced lower peak temperatures.

References

[1] A. Bentur, K. Kovler, Evaluation of early age cracking characteristics in cementitious systems, Mater. Struct. 36 (2003) 183–190.
[2] F. Barre, P. Bisch, D. Chauvel, et al., Control of Cracking in Reinforced Concrete Structures: Research Project CEOS.Fr, Wiley, 2016.
[3] F. Kanavaris, M. Azenha, D. Schlicke, K. Kovler. "Longitudinal restraining devices for the evaluation of structural behaviour of cement-based materials: The past, present and prospective trends", Strain (Wiley), 2020 [Article in Press].
[4] F. Kanavaris, M. Azenha, M. Soutsos, K. Kovler, Assessment of behaviour and cracking susceptibility of cementitious systems under restrained conditions through ring tests: A critical review, Cem. Concr. Compos. 95 (2019) 137–153.
[5] F. Kanavaris, "Early age behaviour and cracking risk of concretes containing GGBS", PhD Thesis, Queen's University Belfast, Belfast, UK, 2017.
[6] M. Azenha. "Numerical simulation of the behaviour of concrete since its early ages", PhD Thesis, University of Minho, Guimaraes, Portugal, 2009.
[7] B. Klemczak, A. Knoppik-Wróbel, Reinforced concrete tank walls and bridge abutments: Early age behaviour, analytic approaches and numerical models, Eng. Struct. 84 (2015) 233–251.
[8] I. Sfikas, C. Makaginsar, J. Banks, D. Gibson, A. Douglas, I. Gibb. "Developing a Common Approach to using Eurocode 2 for Early Thermal Effects and Crack Control – Process and Lessons learnt". In: Proceedings of the 2nd International RILEM/COST Conference on Early Age Cracking and Serviceability in Cement-based Materials and Structures - EAC2, 12–14 September, ULB-VUB, Brussels, Belgium, 2017.
[9] F.U.A. Shaikh, "Effect of cracking on corrosion of steel in concrete", Int. J. Concr. Struct. Mater., 12(3), 2018 [Article in press].
[10] P.B. Bamforth. "Early age thermal crack control in concrete", CIRIA C660, London, 2007.
[11] P.B. Bamforth. "Control of cracking caused by restrained deformation in concrete", CIRIA C766, London, 2018.
[12] M. Briffaut, F. Bendoudjema, G. Nahas, J.M. Torrenti, A thermal active restrained shrinkage ring test to study the early age concrete behaviour of massive structures, Cem. Concr. Res. 41 (1) (2011) 56–63.
[13] H.A. Algaifi, S.A. Bakar, A.R.M. Sam, et al., Numerical modeling for crack self-healing concrete by microbial calcium carbonate, Constr. Build. Mater. 189 (2018) 816–824.
[14] J. Ingham, D. Leek. "Forensic engineering of construction materials: lessons learnt from disputes." Proceedings of the Institution of Civil Engineers: Forensic Engineering, 170, Issue FE1, 2016, pp. 33-44.
[15] I.P. Sfikas, J. Ingham, J. Baber. "Using finite-element analysis to assess the thermal behaviour of concrete structures", Concrete, London, February, 2017, pp. 50-52.
[16] A. Knoppik-Wrobel. "Analysis of early age thermal-shrinkage stresses in reinforced concrete walls", PhD Thesis, Silesian University of Technology, Poland, 2015.
[17] A. Jedrzejewska, F. Kanavaris, M. Zych, D. Schlicke, M. Azenha, Experiences on early age thermal cracking of wall-on-slab concrete structures, Structures 27 (2020) 2520–2549, https://doi.org/10.1016/j.istruc.2020.06.013.
[18] Z. Bofang, Thermal Stresses and Temperature Control of Mass Concrete, Butterworth-Heinemann, 2013.
[19] M. Azenha, R. de Lameiras, S. Sousa, J. Barros, Application of air cooled pipes for reduction of early age cracking risk in a massive RC wall, Eng. Struct. 62–63 (2014) 148–163.
[20] M. Soutsos, A. Hatzitheodorou, J. Kwasny, F. Kanavaris, Effect of in situ temperature on the early age strength development of concretes with supplementary cementitious materials, Constr. Build. Mater. 103 (2016) 105–116.
[21] J. Conceicao, R. Faria, M. Azenha, F. Mamede, F. Souza, Early age behaviour of the concrete surrounding a turbine spiral case: Monitoring and thermo-mechanical modelling, Eng. Struct. 81 (2014) 327–340.

[22] D. Schlicke, F. Kanavaris, R. Lameiras, M. Azenha. "On-site monitoring", in: Fairbairn, E. M. R. and Azenha, M. (eds) "Thermal Cracking of Massive Concrete Structures", State of the Art Report of the RILEM Technical Committee 254-CMS, Springer, 2019, pp. 307-355.
[23] E.M.R. Fairbairn, M. Azenha. (eds) "Thermal Cracking of Massive Concrete Structures", State of the Art Report of the RILEM Technical Committee 254-CMS, Springer, 2019.
[24] B. Klemczak, Modeling thermal-shrinkage stresses in early age massive concrete structures – Comparative study of basic models, Arch. Civ. Mech. Eng. 14 (4) (2014) 721–733.
[25] Jaroslav Keil (ed.), "Výstavba vodního díla Orlík. Sborník statí (The Construction of Orlik dam)", Praha 1967 [in Czech].
[26] Portland Cement Association, "Concrete Information: Ettringite formation and the performance of concrete", PCA IS 417, 2011.
[27] H.F.W. Taylor, C. Famy, K.L. Scrivener, Delayed ettringite formation, Cem. Concr. Res. 31 (5) (2001) 683–693.
[28] A. Pavoine, X. Brunetaud, L. Divet, The impact of cement parameters on Delayed Ettringite Formation, Cem. Concr. Compos. 34 (4) (2012) 521–528.
[29] L. Divet, A. Pavoine. "Delayed ettringite formation in massive concrete structures: An account of some studies of degraded bridges", in: International RILEM TC 186-SA Workshop on Internal Sulfate Attack and Delayed Ettringite Formation, 4-6 September 2002, Villars, Switzerland.
[30] IFFSTAR Techniques and Methods: Recommendations for preventing disorders due to delayed ettringite formation, 2018.
[31] I.P. Sfikas, J. Ingham, J. Baber, Simulating thermal behaviour of concrete by FEA: state-of-the-art review, Proc. Inst. Civ. Eng. Constr. Mater. 171 (CM2) (2018) 59–71, https://doi.org/10.1680/jcoma.15.00052.
[32] American Concrete Institute, "116R-00: Cement and Concrete Terminology", Reported by ACI Committee 116, 2000.
[33] F.-J. Ulm, O. Coussy, What is a "massive" concrete structure at early ages? Some dimensional arguments, J. Eng. Mech. 127 (5) (2001).
[34] T. Honorio, B. Bary, F. Bendoudjema, Evaluation of the contribution of boundary and initial conditions in the chemo-thermal analysis of a massive concrete structure, Eng. Struct. 80 (2014) 173–188.
[35] American Concrete Institute, "207.2R-07 Report on Thermal and Volume Change Effects on Cracking of Mass Concrete", Report of the ACI Committee 207, USA, 2007.
[36] G. De Schutter, L. Taerwe, Estimation of early age thermal cracking tendency of massive concrete elements by means of equivalent thickness, ACI Mater. J. 93 (5) (1996) 1–6.
[37] K. Flaga. Naprężenia własne termiczne typu "makro" w elementach i konstrukcjach z betonu (Macro self-induced thermal stresses in concrete elements and structures), Monograph 106 of Cracow Technical University, 1990 (in Polish).
[38] B. Klemczak, M. Batog, Heat of hydration of low-clinker cements. Part I. Semi-adiabatic and isothermal tests at different temperature, J. Therm. Anal. Calorim. 123 (2) (2016) 1351–1360.
[39] Portland Cement Association, "Concrete technology today – Portland cement, concrete and heat of hydration", Volume 18, Number 2, July 1997, 8 p.
[40] P. Bamforth. "Concreting large-volume (mass) pours", in: Advanced Concrete Technology 3: Processes, edited by Newman, J. and Choo, B.S. Elsevier, 2003, pp. 13/1-13/46.
[41] M. Soutsos, A. Hatzitheodorou, F. Kanavaris, J. Kwasny, Effect of temperature on the strength development of mortar mixes with fly ash and GGBS, Mag. Concr. Res. 69 (15) (2017) 787–801.
[42] L. Lacarrière, A. Knoppik, W.R.L. da Silva, T. Honorio, V. Šmilauer, S. Asamoto, E. M.R. Fairbairn, "Hydration and Heat Development", in: Fairbairn, E. M. R. and Azenha, M. (eds) "Thermal Cracking of Massive Concrete Structures", State of the Art Report of the RILEM Technical Committee 254-CMS, Springer, 2019, pp. 13-46.
[43] M. Azenha, I. Sfikas, M. Wyrzykowski, S. Kuperman, A. Knoppik. "Temperature control", in: Fairbairn, E. M. R. and Azenha, M. (eds) "Thermal Cracking of Massive Concrete Structures", State of the Art Report of the RILEM Technical Committee 254-CMS, Springer, 2019, pp. 153-179.
[44] J. Gajda, M. Vangeem, Controlling temperatures in mass concrete, Concr. Int. 24 (2002) 58–62.
[45] A. Arguez, R.S. Vose, The definition of the standard WMO climate normal: The key to deriving alternative climate normals, Bull. Am. Meteorol. Soc. 92 (2011) 699–704.
[46] D. Serna, P.J.M. Monteiro, Cathedral of our lady of the angels, Concr. Int. (2001) 26–33.
[47] M. Azenha, R. Faria, Temperatures and stresses due to cement hydration on the R/C foundation of a wind tower—A case study, Eng. Struct. 30 (9) (2008) 2392–2400.
[48] R. Faria, M. Azenha, J.A. Figueiras, Modelling of concrete at early ages: Application to an externally restrained slab, Cem. Concr. Compos. 28 (6) (2006) 572–585.
[49] M. Soutsos, F. Kanavaris, A. Hatzitheodorou. "Critical analysis of strength estimates from maturity functions", Case Stud. Constr. Mater., 9, 2018.
[50] J.L. Poole, K.A. Riding, M.C.G. Juenger, K.J. Folliard, A.K. Schindler, "Effects of supplementary cementitious materials on apparent activation energy", J. ASTM Int., Vol. 7, No. 9, 2010.
[51] M.A.A. Elsageer, "Early age strength development of fly ash mixes as affected by temperature", PhD Thesis, University of Liverpool, Liverpool, UK, 2011.
[52] K. Riding, A. Schindler, P. Pesek, T. Drimalas, K. Folliard. "ConcreteWorks V3 Training/User Manual", 0-6332-P1, The University of Texas at Austin, Centre for Transportation Research, April 2017.
[53] J. Červenka, V. Červenka, R. Pukl. "Application of global safety formats from model code 2010 for design and structural assessment by nonlinear analysis", in: Improving Performance of Concrete Structures – The 4th International fib Congress, Universities Press, Mumbai, India, 2014, pp. 695-706.
[54] Z.P. Bažant, S. Baweja. "Creep and shrinkage prediction model for analysis and design of concrete structures – Model B3" Materials and Structures 28, 1995, pp. 357-365, 415-430, 488-495, with Errata in 29, 1996, p. 126.
[55] Z.P. Bažant, S. Baweja, Short form of creep and shrinkage prediction model B3 for structures of medium sensitivity, Mater. Struct. 29 (1996) 586–593.
[56] EN 1992-1-1:2004+A1:2014 – Eurocode 2: Design of concrete structures. General rules and rules for buildings.
[57] N.J.C. Fozein Kwanke, E.A.B. Koenders, W.J. Bouwmeester-van den Bos, J.C. Walraven, Concrete armour units for breakwaters, Concr. Int. 31 (10) (2009) 34–40.
[58] N.J.C. Fozein Kwanke, "Concrete amour units for breakwaters", MSc Thesis, TU Delft, The Netherlands, 2007.
[59] J. Ingham, D. Collery, I.P. Sfikas, M. Badger, Failure of coastal protection concrete armour units due to alkali–silica reaction, Proc. Inst. Civ. Eng. Marit. Eng. 169 (MA3) (2016) 115–123, https://doi.org/10.1680/jmaen.2015.32.
[60] A.J. Edwards. "Early thermal cracking of mass concrete footings on bridges in coastal environment", MSc Thesis, North Carolina State University, USA, 2013.
[61] C.P. Bobko, A.J. Edwards, R. Seracino, P. Zia, Thermal cracking of mass concrete bridge footings in coastal environments, J. Perform. Constr. Facil. 29 (6) (2015).
[62] ACI 301-10: Specifications for structural concrete, Report by ACI committee 301, 2010.
[63] R. Malm, A. Ansell, Cracking of concrete buttress dam due to seasonal temperature variation, ACI Struct. J. 108 (1) (2011) 13–22.
[64] H. Eriksson. "Investigation and rehabilitation of the Storfinnforsen dam", ICOLD 18th International Congress on Large Dams, V. 1, Q68, R19, 1994, pp. 247-259.
[65] A. Fahlén, L. Näslund, "Cracks at Storfinnforsen Concrete Dam—Mapping and Analysis," Division of Structural Engineering, Luleå University of Technology (LTU), Luleå, Sweden, 1991, 89 pp. (in Swedish)
[66] E.I. Funahashi Jr, S.C. Kuperman. "Study of thermal cracking in the spillway of a small hydropower plant", in: VII Simposio sobre Pequenas e Medias Centrais Hidreletricas, CBDB (Brazilian Committee on Dams), Sao Paolo, in Portuguese, 2010.
[67] The Concrete Society, "Guide to the design of concrete structures in the Arabian Peninsula", CS 163, Surrey, UK, 2009.
[68] ACI 305.1-14: Specification for hot weather concrete, Report by ACI Committee 305, 2014.
[69] Itaipu Binacional Website. Available at https://www.itaipu.gov.br/en. [Accessed on October 20th, 2018].
[70] J.A. Rosso, C. Piasentin, "Studies on the cracking of the buttress dam of Itaipu" XXII Simpósio Nacional de Grandes Barragens, CBDB (Brazilian Committee on Dams), Tema III, São Paulo, 1997.
[71] F.R. Andriolo, I. Betioli, Itaipu Project-concrete works: Development, Control, Quality, Durability 40 Years later, Editora Cubo, São Carlos, 2015.
[72] I. Betioli, S.N. Sá, A.S. Fiorini. "Criteria for control and survey of the cracking of the buttress dam of Itaipu." XXII Simpósio Nacional de Grandes Barragens, CBDB (Brazilian Committee on Dams).Tema III, São Paulo, 1997.
[73] G.P. Valentim, Thermal analysis of Itaipu dam during construction, M.Sc. thesis, COPPE/UFRJ, Civil Engineering Department, 2019.
[74] E. Fairbairn, M.M. Silvoso, E.A.B. Koenders, F.L.B. Ribeiro, R.D. Toledo Filho, Thermo-chemo-mechanical cracking assessment for early age mass concrete structures, Concr. Int. 34 (2012) 30–35.
[75] E. Fairbairn, M.M. Silvoso, F.L.B. Ribeiro, R.D. Toledo Filho, Determining the adiabatic temperature rise of concrete by inverse analysis: case study of a spillway gate pier, Eur. J. Environ. Civ. Eng. 21 (3) (2017) 272–288.
[76] G. Bertagnoli, G. Mancini, F. Tondolo, Early age cracking of massive concrete piers, Mag. Concr. Res. 63 (10) (2011) 723–736.